



**Politecnico  
di Torino**

**UNIVERSITY  
OF TWENTE.**

---

**Vibration Analysis and Testing of a Satellite  
Structure during its Launch and In-flight Stages**

---

**Hapuhennedige Sachith Warnakulasuriya**

University dissertation  
to obtain the academic degree

Master of Science in Mechanical Engineering  
(*Laurea Magistrale in Ingegneria Meccanica*)

from

**Politecnico Di Torino**

**Main Supervisor**

Prof. Dario Di Maio  
University of Twente, Netherlands

**Co-supervisor**

Prof. Alessandro Fasana  
Politecnico Di Torino, Italy

Academic Year: 2021

# Abstract

---

The success of a Satellite Launch mission takes into account many factors to consideration with a long planning and a designing procedure. Each phase of the launch vehicle in-flight from launch to reaching the target destination in space is precisely designed and executed. During this process of actually designing a satellite launch the effect of vibrations and its inherent failure and damage mechanics are closely looked upon.

When analysing the vibrations affecting the launch vehicle and the satellite in the payload, we closely look at what type of external forces affect the satellite varying from Acoustic pressures, Structure-borne vibrations to Aerodynamic excitation. This analysis is provided in the initial part of this thesis with a detailed insight to random vibration.

Following on, the author moves to the critical topic of vibration testing of the satellite under the previously analysed external excitation. The forces experienced by the launch vehicle is mainly multi directional while having free boundary conditions. However, in the existing analysis of vibration testing, most of the test methods use single or bi-axial excitation with a high impedance fixture with no attention to the load path. Hence, the current test methods fail to indicate the actual failure modes as observed in-flight and hence will eventually result in high factors of safety driving the production costs higher. After an in detail industrial case study, the author identified a new novel method as suggested in [Dab14] as a solution for vibration testing of critical structures in Aerospace applications. This method is analysed in-depth and a comparison between the exiting testing methods is made.

Physical Vibration Testing, as mentioned above is very important to understand the behavior of structures under different loading conditions. However, the advancement of computer technologies and methods of numerical discretisation have paved way towards computer based mechanical simulations to properly analyse the dynamic characteristics of structures under consideration. The author looks closely to these methods as a step away from physical vibration testing.

Using the softwares ANSYS APDL, ANSYS MECHANICAL and MATLAB the

behavior of a satellite in the payload of a space launch vehicle under different loading conditions is studied. A special attention is given to the critical components of the satellite which are the solar panels and the satellite antenna. These components are modelled using ANSYS MECHANICAL and various mechanical simulations are done which include modal analysis, harmonic analysis and random vibration analysis. The obtained results reveal valuable information about the frequency levels where the designed structure indicate resonance and hence this data can be used in the design process of the space vehicle with the satellite in the payload to avoid these resonances by making structural modification or by using vibration isolation.

In addition to this analysis, a detailed comparison was made to understand the best set estimate of the frequency response function in relation to noise and errors in the input and output. This step was crucial when designing the MATLAB operations to convert the obtained time domain data to indicate the behavior in the frequency domain with a high level of accuracy.

# Acknowledgments

---

Firstly, I'd like to express my thanks to my patient and supportive supervisor **Professor Dario Di Maio** who has supported me throughout this research project. His help and guidance through the weekly meetings to discuss the critical tasks of the Research Project was a catalyst to complete this research with utmost precision that I was capable of.

In addition, a special mention is given to the **Research team affiliated to the Dynamics Based Maintenance group** for the immense support and guidance throughout my tenure as a MSc. Researcher based in the University of Twente.

Also, my co-supervisor in my Alma-mater Politecnico Di Torino, **Professor Alessandro Fasana** for his support to make my transition to the University of Twente an easier process.

Last but not least, my supportive Father **Jayalath Warnakulasuriya** and my loving mother **Kalyani Warnakulasuriya** for their immense support through every means humanly possible.

# List of Figures

---

1.1	The 2 figures show the Atlas V 401 Launch Vehicle . . . . .	2
1.2	Six Degrees of Freedom Dynamic Test System in the Johnson Space Center in USA . . . . .	6
1.3	General Vibration Laboratory in Johnson Space Center . . . . .	7
1.4	Thin solid plate of 100mmX200mmX2mm ( <b>material-structural steel</b> ) . . . . .	9
1.5	Meshed thin plate using Four node rectangular shell elements in ANSYS . . . . .	9
1.6	A thin solid plate with boundary conditions applied . . . . .	9
1.7	The total deformation of the thin plate after a simulation time of 1 second . . . . .	9
2.1	A Simple Pendulum in motion depicted with a view on Kinetic and Potential Energy . . . . .	11
2.2	Image of a patient's colon taken using an ultrasonic probe . . . . .	12
2.3	Tacoma Narrows bridge collapse in 1940 due to wind induced forced vibration . . . . .	13
2.4	Mode shapes 1 at frequency 22.755 Hz . . . . .	14
2.5	Mode shapes 2 at frequency 90.44 Hz . . . . .	14
2.6	Mode shapes 3 at frequency 142.44 Hz . . . . .	15
2.7	Mode shapes 4 at frequency 398.19 Hz . . . . .	15
2.8	Mode shapes 5 at frequency 555.49 Hz . . . . .	15
2.9	Mode shapes 6 at frequency 593.7 Hz . . . . .	16
2.10	Examples of Systems with a Single Degree of Freedom : A spring-mass-damper system and a simple pendulum . . . . .	16
2.11	Examples of Systems with Multi Degrees of Freedom : A spring-mass-damper system with 4 degrees of Freedom and a double pendulum with 2 degrees of freedom . . . . .	16
2.12	Course meshed cantilever beam . . . . .	17
2.13	Fine meshed cantilever beam . . . . .	17
2.14	Spring mass damper system under forced vibration . . . . .	18

2.15	Free body diagram of a spring mass damper system . . . . .	18
2.16	Multi degrees of freedom system excited with two base exciters	19
2.17	Machine in operation which is fixed using bolts without vibration isolation . . . . .	23
2.18	Machine in operation connected to a table through vibration isolation springs . . . . .	23
2.19	Transmissibility of a single degree of freedom system with $\zeta =$ $0.3, \zeta = 0.4, \zeta = 0.5, \zeta = 0.6, \zeta = 0.7, \zeta = 0.8$ . . . . .	24
3.1	Satellite in space which has free boundary conditions . . . . .	26
3.2	Satellite in-flight with mechanical attachment to the launch vehicle	27
3.3	Acoustic vibration environment of a Rocket Launch [Pan14] . .	29
3.4	Electrodynamic Shaker conducting a classical vibration test . .	30
3.5	Model of a Rocket suspended by soft elastics replicating free boundary conditions [Dab14] . . . . .	33
3.6	Impedance Matched Test of a 5 DOF freedom system with 3 shakers to generate excitation and 3 accelerometers to take readings	34
3.7	Resulting time domain plot of M1 . . . . .	36
3.8	FRF Magnitude plots obtained from the data taken from shaker measurements and accelerometer readings . . . . .	36
3.9	FRF Phase Plot obtained from the data taken from shaker Q1 measurements and accelerometer A1 readings . . . . .	36
4.1	A time domain plot of a non-deterministic signal generated in MATLAB . . . . .	38
4.2	A random process with 3 random functions . . . . .	39
4.3	A time domain function indicated by equation 4.7 . . . . .	42
4.4	The frequency domain plot of equation 4.7 . . . . .	42
4.5	The effects of noise on FRF measurements . . . . .	44
4.6	Comparison between $H_1(\omega)$ and $H(\omega)$ when there is noise in the input signal . . . . .	46
4.7	Comparison between $H_2(\omega)$ and $H(\omega)$ when there is noise in the input signal . . . . .	46
4.8	Comparison between $H_1(\omega)$ and $H(\omega)$ when there is noise in the output signal . . . . .	47
4.9	Comparison between $H_2(\omega)$ and $H(\omega)$ when there is noise in the output signal . . . . .	47

4.10	White Noise Input . . . . .	48
4.11	Autocorrelation function of the White Noise Input . . . . .	49
4.12	Power Spectral Density of the White Noise Input . . . . .	49
5.1	Replication of a Satellite with Antenna mounted on a Single Axis Exciter . . . . .	51
5.2	Satellite with Antenna system modelled in ANSYS . . . . .	52
5.3	Mode Shape for frequency 767.74 Hz of the Satellite with Antenna system modelled in ANSYS . . . . .	53
5.4	Mode Shape for frequency 1191.3 Hz of the Satellite with Antenna system modelled in ANSYS . . . . .	54
5.5	Discretized model of a cylinder as depicted in ANSYS . . . . .	55
5.6	Mode Shape of Cylinder at 829.507Hz . . . . .	56
5.7	Mode Shape of Cylinder at 854.651Hz . . . . .	56
5.8	Mode Shape of Cylinder at 1079.75Hz . . . . .	57
5.9	Mode Shape of Cylinder at 1108.85Hz . . . . .	57
5.10	FRF Amplitude plot of the resulting Harmonic Analysis . . . . .	58
5.11	FRF Phase plot of the resulting Harmonic Analysis . . . . .	58
5.12	Construction of a Solar Panel . . . . .	59
5.13	Discretized model of the Solar Panel developed in SOLIDWORKS . . . . .	60
5.14	Mode Shape 1 at 132.97Hz . . . . .	61
5.15	Mode Shape 2 at 249.907Hz . . . . .	62
5.16	Mode Shape 3 at 404.16Hz . . . . .	62
5.17	Mode Shape 4 at 424.97Hz . . . . .	63
5.18	Mode Shape 5 at 546.56Hz . . . . .	63
5.19	Mode Shape 6 at 668.43Hz . . . . .	64
5.20	Power Spectral Density of the Acceleration applied in the -Y direction on the solar panel surface . . . . .	64
5.21	Response Power Spectral Density of a Point on the free end of the Solar Panel . . . . .	65
5.22	Amplitude plot of the Frequency Response Function . . . . .	66
5.23	Phase plot of the Frequency Response Function . . . . .	66
5.24	Longitudinal acceleration in US Discovery space shuttle,in STS- 121 mission . . . . .	67
5.25	The thin plate simulated in ANSYS APDL . . . . .	67
5.26	Description of a Step Input . . . . .	68

5.27	Response of a point on the Thin Plate for 10 seconds . . . . .	69
5.28	Response of a point on the Thin Plate for the initial 2 seconds .	69
5.29	Description of a Ramped input . . . . .	70
5.30	Response of a point on the Thin Plate for 10 seconds . . . . .	70
5.31	Response of a point on the Thin Plate in the last 8 seconds . . .	71

# List of Tables

---

1.1	Sources of launch vehicle environments[Younis 2005] . . . . .	1
1.2	Vibration Testing Apparatus in Johnson Space Center . . . . .	7
2.1	Natural Frequencies of the Cantilever Beam . . . . .	14
5.1	Material Properties of Structural Steel used for modelling the system in ANSYS . . . . .	51
5.2	Cylinder Properties of the modelled system in ANSYS . . . . .	51
5.3	Modal Frequencies of the Satellite Body with Antenna Structure	53
5.4	Modal Frequencies of the Cylinder . . . . .	55
5.5	Properties of the Material used in the Solar Panel . . . . .	60
5.6	Modal Frequencies in the range 100Hz – 700Hz of the Solar Panel developed in ANSYS . . . . .	61

# Contents

---

<b>Abstract</b>	<b>ii</b>
<b>Acknowledgments</b>	<b>iv</b>
<b>Contents</b>	<b>x</b>
<b>1 Introduction</b>	<b>1</b>
1.1 Loads on the spacecraft structure during launch and in-flight phases . . . . .	1
1.2 Vibration Testing of Space Structures . . . . .	3
1.2.1 Environment Test . . . . .	4
1.2.2 Environments for which we design vibration tests . . . . .	4
1.2.3 Environment Capture trials . . . . .	5
1.2.4 Test Specifications . . . . .	5
1.2.5 Vibration Measuring Apparatus used by The Johnson Space Center(JSC)in USA . . . . .	6
1.3 Simulation Models based on Finite Element Analysis . . . . .	9
1.3.1 Finite Element Method . . . . .	9
1.3.2 Comparison between Vibration Test and Finite Element Simulations . . . . .	10
<b>2 Theory of Mechanical Vibrations</b>	<b>11</b>
2.1 Mechanical Vibrations . . . . .	11
2.2 Natural frequency,Mode Shapes and Resonance . . . . .	13
2.3 Degrees of Freedom . . . . .	16
2.3.1 Discrete and Continuous Systems . . . . .	17
2.4 Equations of Motion . . . . .	17
2.5 Modal Analysis . . . . .	20
2.5.1 Modal Analysis for a structure in free undamped vibration	21
2.6 Vibration Damping . . . . .	21
2.6.1 Vibration Isolation . . . . .	22

<b>3</b>	<b>IMMAT(Impedance Matched Multi Axis Testing)</b>	<b>25</b>
3.1	Introduction to IMMAT . . . . .	25
3.2	Classical Vibration test methods . . . . .	26
3.2.1	Boundary Conditions . . . . .	26
3.2.2	Excitation Environments . . . . .	27
3.3	Mounting impedance . . . . .	31
3.3.1	Advanced Fixtures . . . . .	31
3.4	Impedance Matched Multi Axis Testing . . . . .	32
3.5	Numerical Simulation of a Impedance-Matched Multi Axis Test	33
3.5.1	Introduction . . . . .	33
3.5.2	System Parameters,Mass Matrix and Stiffness Matrix . .	34
3.5.3	Time Domain Response of the System . . . . .	35
3.5.4	Frequency Response Functions of the system . . . . .	35
3.6	Concluding remarks on Impedance Matched Multi Axis Test . .	37
<b>4</b>	<b>Introduction to Random Vibration</b>	<b>38</b>
4.1	Introduction . . . . .	38
4.2	Correlation function of a Random Process . . . . .	39
4.2.1	Stationary Random Processes and Ergodicity . . . . .	40
4.3	Random Process Analysis in the Frequency Domain . . . . .	41
4.3.1	Power Spectral Densities . . . . .	42
4.4	Frequency Response Function . . . . .	43
4.5	A Random Excitation Signal . . . . .	48
<b>5</b>	<b>Vibration Analysis of a Satellite</b>	<b>50</b>
5.1	Introduction . . . . .	50
5.2	Mode Shapes of a Satellite Body with Antenna Structure . . . . .	50
5.3	Mode Shapes of the Cylinder available in the laboratory Model depicted in figure 5.1 . . . . .	55
5.3.1	Harmonic Analysis of the Cylinder available in the lab- oratory Model depicted in figure 5.1 . . . . .	57
5.4	Vibration Analysis of a Satellite Solar Panel . . . . .	59
5.4.1	Introduction . . . . .	59
5.4.2	Modal Analysis of the Satellite Solar Panel . . . . .	60
5.4.3	Random Vibration Analysis of the modelled solar panel in ANSYS . . . . .	64
5.4.4	Harmonic Vibration Analysis of the solar panel . . . . .	65

5.4.5	Effect of Step vs Ramp Acceleration on a Solar Panel . .	66
<b>6</b>	<b>Conclusions &amp; Outlook</b>	<b>72</b>
	<b>Bibliography</b>	<b>74</b>

## 1.1 Loads on the spacecraft structure during launch and in-flight phases

During the Launch and In-flight stages of a space launch vehicle there are harsh environments created due to vibrations and acoustics. They affect the launch pad, the launch vehicle and its payload the satellite which includes critical structures like the antenna and solar panels.

The noise created during the launch phase and the two minute liftoff and transonic (*speed is lower than the speed of sound*) climb phase generates intense acoustic loads. These acoustic loads are a result of an intense acoustic environment generated by the interaction of the rocket engine exhaust mixing with the atmosphere. In addition to these acoustic loads at liftoff the rocket motors generates an acceleration on the satellite and its payload which impose a large steady state load.

In addition to these loads, at liftoff, there are vibrations generated due to engine shutdowns, wind gusts, and quasi-static loads. These can result in vibration environments of Acoustic, Random, Sine and Shock origins.

Below is a table indicating the environments observed during the ascent profile of a space launch vehicle.

Ascent phase of launch vehicle	Acoustics	Random Vibration	Sine Vibrations	Shock
Liftoff	X	X		
Aerodynamics/Buffer	X	X		
Separation (stage, fairing, spacecraft)				X
Motor burn/Combustion		X	X	

**Table 1.1:** Sources of launch vehicle environments [Younis 2005]

The Maximum loads (*flight limit loads*) at each phase in the life cycle of the



(a) Launch of an Atlas V 401 carrying the Lunar Reconnaissance Orbiter and LCROSS space probes on 18 June 2009.



(b) Atlas V 401 launch system structure

**Figure 1.1:** The 2 figures show the Atlas V 401 Launch Vehicle

launch vehicle and the satellite are used as data to design the components with the consideration of acceptable safety factors.

The Dynamic Mechanical loads that occur during the lifetime of a spacecraft are of a wide variety. They are discussed in detail as below [08] [CMN].

Also, not mentioned in this thesis are the Handling loads, Transportation loads which occur before launch.

- Qualification tests that are required to ensure that the structure satisfies the maximum load limits
  - Sinusoidal vibrations
  - Random vibrations
  - Acoustic pressures
- Dynamic loads during launch
  - Steady state accelerations (inertia loads)
  - Random vibrations
  - Pressure variations
  - Acoustic loads

- Loads following launch
  - Loads due to structural movements(ie. Solar Panels,Antennas,Telescopes)
  - Loads due to collision of space debris/meteorites
  - Zero gravity loads
- Loads on the spacecraft in orbit (In-service loads)
  - Transfer orbit loads
  - Loads due to collision of space debris/meteorites
  - Zero gravity loads
- Steady-state static loads
  - The Propulsion of the engine
  - Wind loads
- Mechanical dynamic loads as a result of unsteady combustion of the engines,turbulent exhaust flows in the rocket and exhaust noise[significant during the initial launch phase]
- Shock loads
  - The separation of launch vehicle from different stages generate the highest shock load
  - Ignition and stopping of engines

As seen above, there are various types of forces and loads applied on the space vehicle structure during its lifetime.So,the next question is to see how we can conduct tests to simulate the above mentioned load conditions in order to ensure that the space vehicle will not fail during its planned service life.Hence, we have to move into the realm of vibration testing of space structures [Pie66].

## 1.2 Vibration Testing of Space Structures

Critical structures, like the launch vehicle and its payload, are those whose failure in service could be catastrophic,leading to significant financial costs and reputation damage.Hence,the safety and performance of these structures must be

qualified using laboratory-based environment tests, with the aim of simulating the **in-service environments**.

A proper vibration test should have two main characteristics as below, in order for it to be an acceptable simulation of the **in-service environments**.

1. The Boundary Conditions of the test environment must match the in-service environment.
2. The load path applied in test environment must match the in-service conditions.

Generally, even in some of the modern day tests these considerations are not met in unison which results in significant over-tests with unrealistic failures occurring in the laboratory environment. Because of this, it results in lengthy and costly delays in the laboratory environment [Dab14].

However, a new novel test approach which satisfies both the above requirements are developed by [Dab14] known as **Impedance-Matched Multi Axis Testing (IMMAT)**. This is a far superior test and will be discussed in detail in chapter 3.

### 1.2.1 Environment Test

An Environment Test is a dynamic test which is used to determine whether a structure will incur any damage, malfunction or deterioration during its service life.

### 1.2.2 Environments for which we design vibration tests

The structure that we are interested in can be in any different type of environment. For example, our space structure before launch is having a high impedance due to structural connections. After its launch and in-flight situations it is having an almost free-free atmospheric environment and when it is in outer space it is in a zero gravity environment with free-free boundary conditions.

These different environments pose various types of dynamic environments like acceleration, blast, mechanical shock, vibration and wind etc., In this thesis we are more considerate about Random and Sinusoidal environmental excitation and its effects.

### 1.2.3 Environment Capture trials

Environment capture trials are done to allow the engineers to understand a structure's dynamic response to its in-service environment.

For example, an Environment Capture Trial for an aircraft can be a situation where accelerometers are placed on critical locations of the aircraft and their readings are used to record its dynamic behavior during a selected number of in-service missions.

The data from these environment capture trials are collated to form a test specification, which is to be replicated in the subsequent laboratory tests to be performed.

### 1.2.4 Test Specifications

Test specifications provides the details of the test to be carried out like the *test severity levels, duration and procedure to be followed during the test*. At many testing facilities a significant amount of time and effort is dedicated to ensure that the test specifications are in-line to the highest degree possible with the methods available at that time. However, still some institutions rely on outdated methods based on standard techniques prescribed in Military Organisations and other standard organisations like the International Standard Organisation (ISO).

Most of the time, test specifications are drawn up with a lack of crucial information like the variability of environment severity, mounting impedance or equipment strength. This lack of crucial information results in the addition of an exaggerated **factor of safety** which results in over-testing.

A Test specification described by Lelanne C. in [Lal10] is said to follow the below criteria

1. If the structure functions correctly during the test, there should be a strong probability that it will function correctly in the real environment. This means that test environments should be at least as severe as the real environment.
2. If the equipment fails during the test, there should be a strong probability that it will fail in operation. The test should not be overly severe.

### 1.2.5 Vibration Measuring Apparatus used by The Johnson Space Center(JSC)in USA

As per [AA], the Johnson Space Center offers a wide variety of tests to evaluate all aspects of structural dynamics, including vibration,vibroacoustics,modal characteristics,sound transmission loss and shock testing. Also the resource [AA] states that the below mentioned services and facilities are available for Vibration testing in the Johnson Space Center.



**Figure 1.2:** Six Degrees of Freedom Dynamic Test System in the Johnson Space Center in USA

#### Services Provided

- Simulations of broadband random vibrations induced in spacecraft by external acoustic pressures
- Sine sweeps to identify resonances
- Broadband random environments that do not simulate mission conditions but are appropriate for precipitating impending failures due to workmanship defects
- Vibration of hazardous test articles, including pressurized systems and explosive materials – vibration in a thermal environment

- Vibroacoustic structural testing to high sound pressure levels of large structures, components, and small subsystems
- Modal characteristics identification
  - Natural frequencies
  - Damping ratios
  - Mode shapes



**Figure 1.3:** General Vibration Laboratory in Johnson Space Center

Facility	Frequency Range	Shaker Size Range	Load Direction	Displacement
General Vibration Laboratory (GVL)	5-3000 Hz	4,000-40,000 lb <sub>f</sub>	x,y, or z	1" to 2" peak-to-peak
Spacecraft Vibration Laboratory (SVL)	5-2000 Hz	50 lb <sub>f</sub> shakers up to 8 x 10,000 lb <sub>f</sub> shakers	x,y, or z	2" peak-to-peak
Hazardous Vibration Test Stand	20 – 2000 Hz	11,000 lb <sub>f</sub> RMS Up to 16,000 lb <sub>f</sub> sine Up to 15,500 lb <sub>f</sub> random	x,y, or z	1" stroke

**Table 1.2:** Vibration Testing Apparatus in Johnson Space Center

### General Vibration Laboratory

The GVL has five primary testbeds; however, unique testbeds can be constructed as necessary to meet a specific test project. Inside the GVL enclosure (removable ceiling panels), the 40,000 lbf shakers for the vertical and horizontal testbeds are mounted to seismic floors. Outside the GVL enclosure are two more testbeds,

an 18,000 lbf vertical testbed and a 20,000 lbf horizontal testbed. The GVL also houses a 8,000 lbf human-rated vibration testbed. The laboratory typically provides testing for subsystems and smaller components from as large as an aircraft rudder to as small as a 4 oz heart rate monitor.

### **Spacecraft Vibration Laboratory**

The SVL was specifically designed for vibration testing of large structures and used for Apollo, Skylab, Space Shuttle, and Space Station tests. It provides a vast array of access platforms to the test articles. Massive test articles can be supported by pneumatic springs and subjected to high-force inputs, which simulate rocket-induced discrete-frequency or random loads with distributed mechanical shakers. Typical testing functions performed include high-force vibration (random and sine), shock vibration, and fixed base and free-free modal testing.

### **Hazardous Vibration Test Stand**

The Hazardous Vibration Test Stand provides for vibration of pressurized systems and explosive materials and vibration within a thermal environment. The test stand supports test articles (including fixture) up to 2,000 lb. Vibration capability includes sine, random, and classical shock.

As seen above, there are various vibration testing done during design and after-design of space structures. Due to the flexibility of testing centers there is a possibility to make the test bespoke to the space structure under observation. However, even with these facilities readily available, the cost of running tests remain significant. Hence, we try to integrate computer based simulations along with physical vibration testing to minimize the cost and time required to give the structure a green light to go into operation.

## 1.3 Simulation Models based on Finite Element Analysis

### 1.3.1 Finite Element Method

**Finite Element Method** is an approach to solve differential equations and boundary value problems. In FEM, we divide the body under consideration into smaller parts called finite elements.

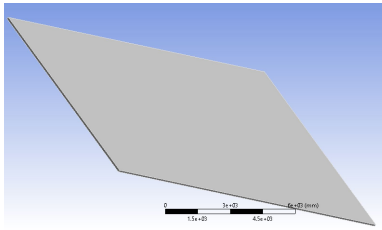


**Figure 1.4:** Thin solid plate of  $100\text{mm} \times 200\text{mm} \times 2\text{mm}$  (material-structural steel)

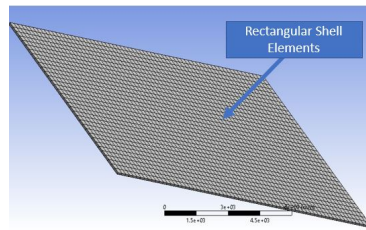


**Figure 1.5:** Meshed thin plate using Four node rectangular shell elements in ANSYS

The set of finite elements in unison is called the mesh. This mesh should be regular and uniform as possible, and the element size should be adequate to meet the precision required. Once the meshing is done, the next step is to apply the required boundary conditions and then to proceed to obtain the solutions [BS16].

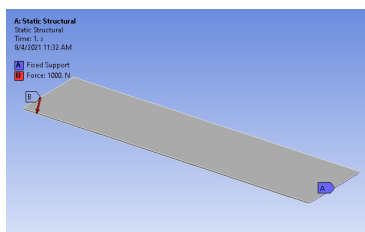


**Figure 1.6:** A thin solid plate with boundary conditions applied

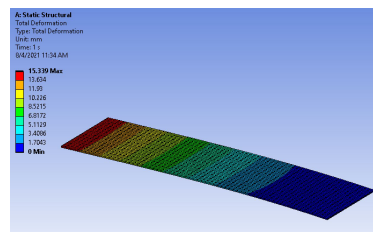


**Figure 1.7:** The total deformation of the thin plate after a simulation time of 1 second

### 1.3.2 Comparison between Vibration Test and Finite Element Simulations

In addition to physical testing, simulation models are also available to predict the behavior of critical structures. These are based on Finite Element Models which run on a theoretically based algorithm to predict the behavior of physical structures. The behavior of these types of models are analysed based on the inherent properties of the system like the Modal Characteristics, or its response to an externally applied load of different frequencies or magnitude values.

Most believe that these simulation models are a low cost alternative to large laboratory based vibration tests. However, this statement is to be made into argument based on the case involved. For example, complex analytical simulations require supercomputers along with expensive FEM software and Analyst time. This is the case in the aerospace industry and defence applications in the modern era.

However, the author of this thesis believe that the best way to predict the behavior of the vibratory response of structures is to use simulations and vibration tests in tandem. By this, the author means to first run the simulations to predict the behavior and hence reduce the number of iterations needed for the physical tests, thus reducing the cost of tests and saving precious time [Dab14] [Knu73] [Lal10].

# 2

## Theory of Mechanical Vibrations

---

### 2.1 Mechanical Vibrations

Any motion that repeats itself after an interval of time is called as *Vibration Oscillation* [Rao93]. The motion of a pendulum or a plucked string in a guitar are examples of vibratory motion.

A vibratory system in general has a means of storing kinetic energy (a mass element) along with a means of storing potential energy (elastic element or a spring) along with a damper which dissipates the energy available in the system. During vibration the available potential energy is converted to kinetic energy or vice versa. If there is the availability of damping, the total energy of the system reduces and the vibration amplitude reduces overtime and the system comes to a stop. But, in order to maintain the vibratory motion an external source of energy is always required if there is the presence of damping.

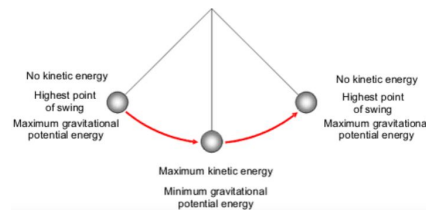


**Figure 2.1:** A Simple Pendulum in motion depicted with a view on Kinetic and Potential Energy

Vibrations in general occur in almost all mechanical systems in some magnitude. It may be a significant factor in consideration or not, it is definitely capable of significantly affecting the structural behavior.

Below are several examples where vibrations can lead to detrimental or catastrophic situations.

- Excessive vibrations during operation of pumps, turbo machinery and



## 2.2 Natural frequency, Mode Shapes and Resonance

If a system, after an initial disturbance is set to vibrate on its own naturally, the frequency with which it oscillates without an external unbalanced force is known as its **Natural Frequency**. The Natural Frequency is also known as the characteristic frequency, fundamental frequency, resonant frequency, resonance frequency and normal frequency.

The deformed shape of the structure at a specific natural frequency of vibration is termed as its **mode shape** of vibration. A given mode shape is a unique characteristic of the respective natural frequency. The term mode shape is also known as normal mode, characteristic mode and fundamental shape.

In the case of Forced vibration, we experience a new phenomenon as described below.

When the natural frequency of the vibrating structure coincides with the frequency of excitation of the external force/load applied, then a phenomenon called **resonance** occurs. At resonance, the structure is said to vibrate violently with excessive amplitudes. The detrimental effect of the Resonance phenomena that occurs during Forced vibration can be clearly understood by the Tacoma Narrows bridge collapse due to wind-induced vibration which is indicated below.



**Figure 2.3:** Tacoma Narrows bridge collapse in 1940 due to wind induced forced vibration

**Below are some of the Natural Frequencies and Mode shapes of a Cantilever beam with dimensions 40mmX10mmX600mm and material structural steel as produced in Ansys Workbench R2 2021 edition.**

Mode Number	Natural Frequency
1	22.755
2	90.44
3	142.44
4	398.19
5	555.4
6	593.7

Table 2.1: Natural Frequencies of the Cantilever Beam

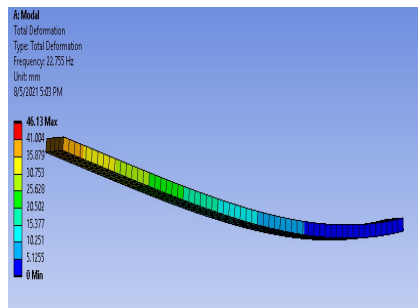


Figure 2.4: Mode shapes 1 at frequency 22.755 Hz

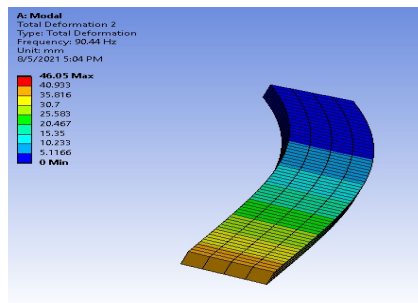


Figure 2.5: Mode shapes 2 at frequency 90.44 Hz

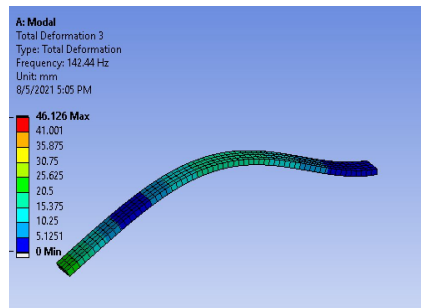


Figure 2.6: Mode shapes 3 at frequency 142.44 Hz

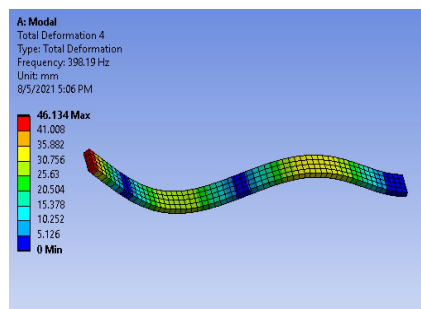


Figure 2.7: Mode shapes 4 at frequency 398.19 Hz

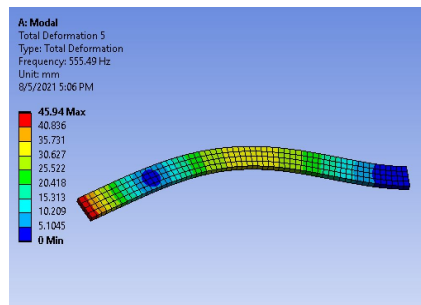


Figure 2.8: Mode shapes 5 at frequency 555.49 Hz

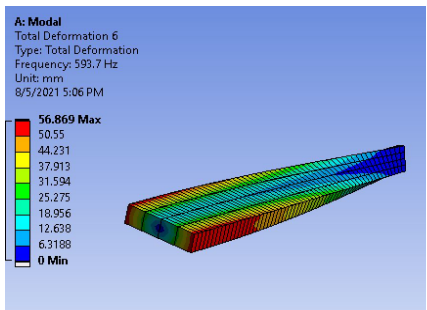


Figure 2.9: Mode shapes 6 at frequency 593.7 Hz

### 2.3 Degrees of Freedom

The minimum number of independent parameters required to determine completely the positions of all parts of a system at any instant of time defines the number of degree of freedom of a system. [Rao93]

Generally, bodies or structures in the real world is said to have an infinite number of degrees of freedom but for the sake of analysis we simplify them down to a finite number of degrees of freedom.

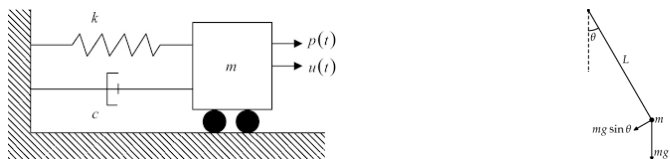


Figure 2.10: Examples of Systems with a Single Degree of Freedom : A spring-mass-damper system and a simple pendulum

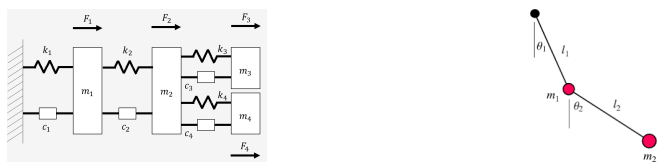


Figure 2.11: Examples of Systems with Multi Degrees of Freedom : A spring-mass-damper system with 4 degrees of Freedom and a double pendulum with 2 degrees of freedom

### 2.3.1 Discrete and Continuous Systems

All systems in practice, as discussed above is said to have an infinite number of degrees of freedom. However, most of the simple systems can be assumed to have a finite number of degrees of freedom and solved for with acceptable accuracy.

Systems that have an infinite number of degrees of systems are called as **continuous systems** or **distributed systems** while the systems with a finite number of degrees of freedom are called as **discrete systems** or **lumped parameter systems**.

Below indicates a cantilever beam which in practise is said to have an infinite number of degrees of freedom. But, for the sake of solving the system we discretize it to have a finite number of degrees of freedom with the assumption that the required accuracy is obtained. Generally, greater the number of degrees of freedom the higher is the accuracy. But, as the degrees of freedom increase the computation time increase and also the cost associated with computation due to the requirement of faster and superior processors [BB04].

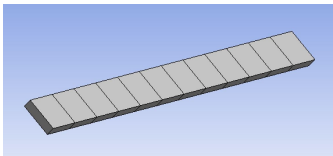


**Figure 2.12:** Course meshed cantilever beam

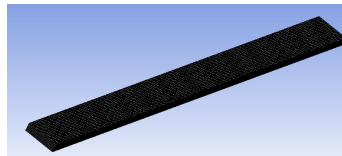


**Figure 2.13:** Fine meshed cantilever beam

## 2.4 Equations of Motion

The most straightforward method of analysing a dynamic system is to use the equations of motion. Hence, to give an insight to this approach to the reader, the author is going to introduce a single degree of freedom (SDOF) model. The model indicated consists of a spring, a damper and a mass. For simplicity, we assume that the spring and the damper is both massless and the mass  $\mathbf{m}$  moves only vertically and a time dependent vertical force  $\mathbf{F}(\mathbf{t})$  acts on the mass  $\mathbf{m}$ .

By Analysing the free body diagram in figure 2.15 and using Newton's laws, we can derive the below equation 2.1.

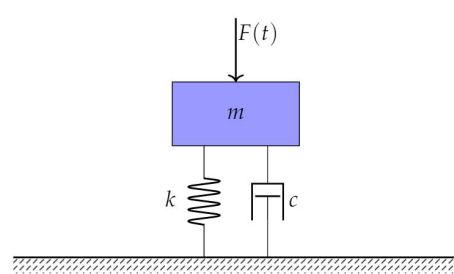


**Figure 2.14:** Spring mass damper system under forced vibration

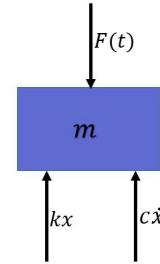


**Figure 2.15:** Free body diagram of a spring mass damper system

$$F(t) - m \frac{d^2x}{dt^2} - c \frac{dx}{dt} - kx = 0 \tag{2.1}$$

By re-organizing the terms of the above equation, we can derive the **equation of motion for a SDOF model** as below in equation 2.2:

$$m \frac{d^2x}{dt^2} + c \frac{dx}{dt} + kx = F(t) \tag{2.2}$$

For a more sophisticated dynamic system it is necessary to include more than one degree of freedom to describe the dynamic behavior. Because of this we move into Multi Degree of Freedom (MDOF) systems. Even though, the system becomes complex in nature the final resulting equations of motion can be simplified into the below form by applying several assumptions.

$$\mathbf{M} \frac{d^2\mathbf{x}}{dt^2} + \mathbf{C} \frac{d\mathbf{x}}{dt} + \mathbf{K}\mathbf{x} = \mathbf{F}(t) \tag{2.3}$$

In the above equation 2.3,  $\mathbf{M}$  is the mass matrix,  $\mathbf{K}$  is the stiffness matrix,  $\mathbf{C}$  is the damping matrix. Also,  $\mathbf{x}$  is the displacement vector and  $\mathbf{F}(t)$  is the load vector. *If there are  $n$  degrees of freedom in the system, the matrices will have the dimensions  $n \times n$  and the vectors of dimensions  $n \times 1$ .*

**In figure 2.16 is a complex system with Multi Degrees of Freedom which is analysed by the author using Newton’s laws. The Equations of motions obtained are represented below.**

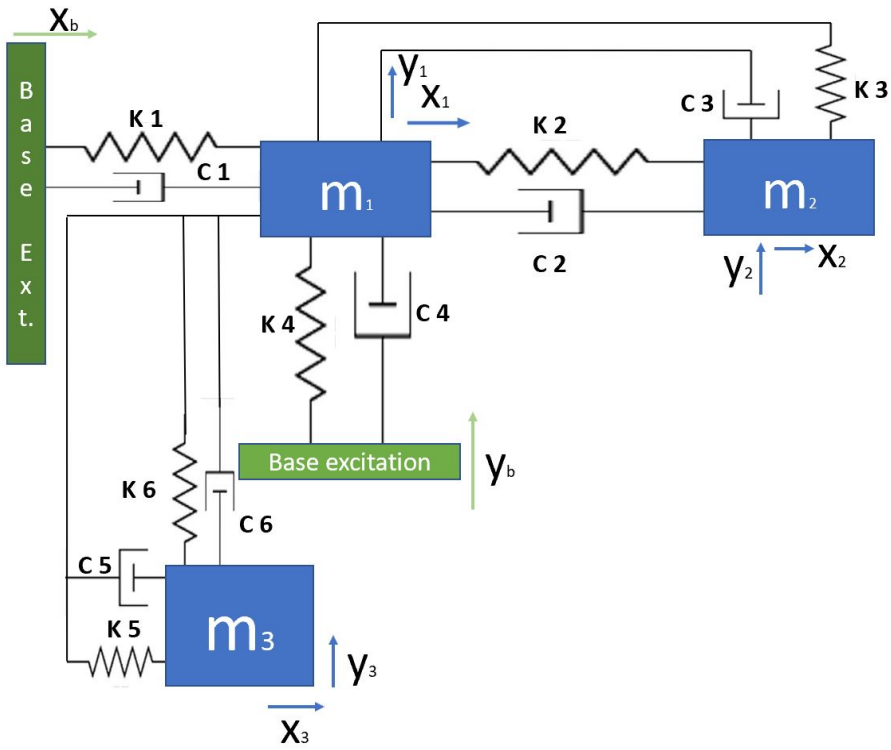


Figure 2.16: Multi degrees of freedom system excited with two base exciters

$$X = \begin{bmatrix} x_1 \\ x_2 \\ x_3 \\ y_1 \\ y_2 \\ y_3 \end{bmatrix} \tag{2.4}$$

$$M = \begin{bmatrix} m1 & 0 & 0 & 0 & 0 & 0 \\ 0 & m2 & 0 & 0 & 0 & 0 \\ 0 & 0 & m3 & 0 & 0 & 0 \\ 0 & 0 & 0 & m1 & 0 & 0 \\ 0 & 0 & 0 & 0 & m2 & 0 \\ 0 & 0 & 0 & 0 & 0 & m3 \end{bmatrix} \quad (2.5)$$

$$K = \begin{bmatrix} (k1 + k2 + k5) & -k2 & -k5 & 0 & 0 & 0 \\ -k2 & k2 & 0 & 0 & 0 & 0 \\ -k5 & 0 & k5 & 0 & 0 & 0 \\ 0 & 0 & 0 & (k4 + k6 + k3) & -k3 & -k6 \\ 0 & 0 & 0 & -k3 & k3 & 0 \\ 0 & 0 & 0 & -k6 & 0 & k6 \end{bmatrix} \quad (2.6)$$

$$C = \begin{bmatrix} (c1 + c2 + c5) & -c2 & -c5 & 0 & 0 & 0 \\ -c2 & c2 & 0 & 0 & 0 & 0 \\ -c5 & 0 & c5 & 0 & 0 & 0 \\ 0 & 0 & 0 & (c4 + c6 + c3) & -c3 & -c6 \\ 0 & 0 & 0 & -c3 & c3 & 0 \\ 0 & 0 & 0 & -c6 & 0 & c6 \end{bmatrix} \quad (2.7)$$

$$F(t) = \begin{bmatrix} k1 & c1 \\ 0 & 0 \\ 0 & 0 \\ 0 & 0 \\ 0 & 0 \\ 0 & 0 \end{bmatrix} \begin{Bmatrix} x_{b1} \\ \dot{x}_{b1} \end{Bmatrix} + \begin{bmatrix} 0 & 0 \\ 0 & 0 \\ 0 & 0 \\ k4 & c4 \\ 0 & 0 \\ 0 & 0 \end{bmatrix} \begin{Bmatrix} y_{b1} \\ \dot{y}_{b1} \end{Bmatrix} \quad (2.8)$$

The **Displacement Vector** of the system is 2.4, the **Mass matrix** of the system is 2.5, the **Stiffness matrix** of the system is 2.6 and the **Damping matrix** of the system is 2.7, the **Load matrix** of the above system is 2.8.

## 2.5 Modal Analysis

**Modal Analysis** is a powerful tool to identify the dynamic characteristics of structures. By using modal analysis we can evaluate the natural frequencies, the

respective mode shapes at the natural frequencies and the damping at these natural frequencies of structures.

### 2.5.1 Modal Analysis for a structure in free undamped vibration

The equation 2.3 reduces to the below form since  $\mathbf{C} = 0$  (the system is *undamped*) and  $\mathbf{F}(\mathbf{t}) = 0$  since the system is in *Free Vibration*.

$$\mathbf{M} \frac{d^2 \mathbf{x}}{dt^2} + \mathbf{K} \mathbf{x} = \mathbf{0} \quad (2.9)$$

To solve the above equation 2.9 we assume a harmonic solution as below in equation 2.10.

$$\mathbf{x}(\mathbf{t}) = \mathbf{A} \cos(\omega t) \Phi + \mathbf{B} \sin(\omega t) \Phi \quad (2.10)$$

In the above equation 2.10 the matrixes A and B are solely dependent on the initial condition  $\mathbf{x}(0)$  and  $\dot{\mathbf{x}}(0)$ .

By differentiating for  $\mathbf{x}(\mathbf{t})$  and substituting in equation 2.9 we obtain the equation for the **eigenvalue problem**.

$$(\mathbf{K} - \omega^2 \mathbf{M}) \Phi = 0 \Leftrightarrow \det(\mathbf{K} - \omega^2 \mathbf{M}) = 0 \quad (2.11)$$

By solving equation 2.11 we can find  $\omega_1, \omega_2, \omega_3, \dots, \omega_n$  which are called the **Natural Frequencies**. By using these natural frequencies and re-substituting them in equation 2.11 we can find the **mode shapes** of the system.

## 2.6 Vibration Damping

Even though, we omitted damping to simplify the analysis for finding the natural frequencies it is an effect present in most systems. Damping is a methodology we use in mathematical models to represent the energy dissipation in structural dynamics. For example, energy is dissipated through damping available in automobile shock absorbers and many vibration-measuring instruments.

If a system undergoes forced vibration, its amplitude of vibration tends to become larger near resonance, if damping is absent in the system. But, the presence of damping mitigates the extensive response levels.

For free vibration, the equation 2.3 can be re-written in the below form.

$$\frac{d^2 \mathbf{x}}{dt^2} + 2\zeta\omega_n \frac{d\mathbf{x}}{dt} + \omega_n^2 \mathbf{x} = 0 \quad \text{where} \quad \omega_n = \sqrt{k/m} \quad , \quad \zeta = \sqrt{c/(2m\omega_n)} \quad (2.12)$$

$\zeta$  is termed as the **damping ratio** and  $\omega_n$  as the **natural frequency for an undamped system**. Moreover, the damping ratio is a system parameter which is denoted by  $\zeta$  and the system can be characterised based on damping as below.

- Undamped System ( $\zeta = 0$ )
- Underdamped System ( $\zeta < 1$ )
- Critically Damped System ( $\zeta = 1$ )
- Overdamped System ( $\zeta > 1$ )

The Solution for the system if it's Underdamped ( $\zeta < 1$ ) is provided below in equations 2.13 and 2.14.

$$x(t) = e^{-\zeta\omega_n t} \left( x(0)\cos(\omega_D t) + \frac{\frac{dx}{dt}\big|_{t=0} + \zeta\omega_n x(0)}{\omega_D} \sin(\omega_D t) \right) \quad (2.13)$$

$$\omega_D = \omega_n(1 - \zeta^2) \quad (2.14)$$

### 2.6.1 Vibration Isolation

Vibration Isolation is the procedure by which the negative and undesirable effects of vibration is reduced. The process of vibration isolation involves the addition of an isolator(a resilient member) between the equipment or payload and the vibration source in order to reduce the dynamic response of the system due to the vibration excitation [OH22]. An isolation system can be active or passive based on the fact that they require external power to function or not.

A passive vibration isolator has a damping member(an energy dissipator) and a resilient member(a member with stiffness).Examples include metal springs,pneumatic springs,cork,felt and elastomer(rubber) springs. An active vibration isolator on the other-hand is comprised of a servomechanism with a sensor,signal processor, and an actuator [WL92].

**In figure 2.17 is indicated a Machine element mounted on a table with bolts. In this scenario there is no vibration isolation provided and the**

force transmitted to the table is significant. However, in figure 2.18 passive vibration isolators with damping and stiffness is provided which acts to reduce the transmitted force.

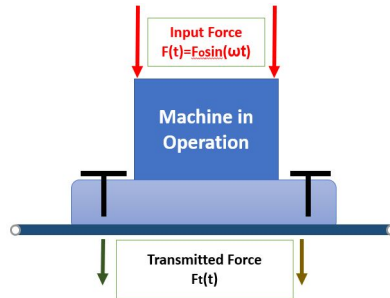


Figure 2.17: Machine in operation which is fixed using bolts without vibration isolation

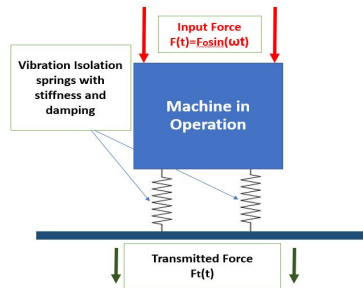


Figure 2.18: Machine in operation connected to a table through vibration isolation springs

The corresponding equations relevant to figure 2.18 follows below in equation 2.15.

$$m \frac{d^2x}{dt^2} + c \frac{dx}{dt} + kx = F(t) \tag{2.15}$$

If the damping is neglected then we can derive the below equation for the vertical motion of the system  $x(t)$ .

$$x(t) = \frac{F_0}{k} \frac{1}{1 - r^2} \sin(\omega t) \quad \text{where} \quad r = \frac{\omega}{\omega_n} \tag{2.16}$$

In the case of no damping, we can say that the force transmitted is  $F_T = kx$ .

In order to define the magnitude of vibration isolation, we introduce a new parameter called **Transmissibility** identified with variable **T** in this thesis. In definition, it is the ratio of the force transmitted over the force applied. The lower the variable **T** higher is the magnitude of vibration isolation involved.

If **Transmissibility** is lower than 1 ( $T < 1$ ) we can say that vibration isolation occurs. For minimum transmissibility or maximum isolation, the excitation frequency should be as much as possible above the natural frequency.

$$T = \left| \frac{F_T}{F_o} \right| = \left| \frac{1}{r^2 - 1} \right| \tag{2.17}$$

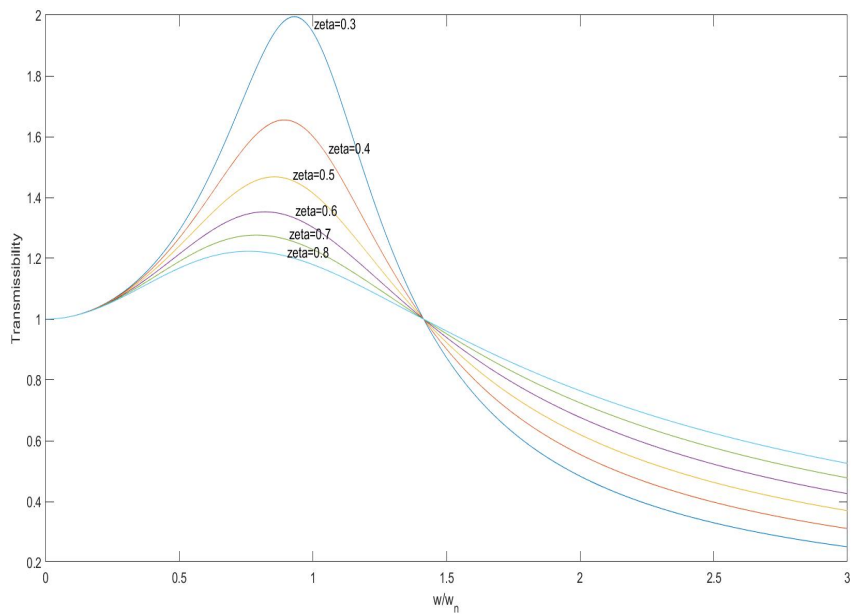


**Figure 2.19:** Transmissibility of a single degree of freedom system with  $\zeta = 0.3, \zeta = 0.4, \zeta = 0.5, \zeta = 0.6, \zeta = 0.7, \zeta = 0.8$

### 3.1 Introduction to IMMAT

There are 3 main types of Environments experienced by a satellite during launch and in-flight stages as below.

- Acoustic excitation
- Aerodynamic excitation
- Structure-borne vibration

The goal of Vibration testing should be to successfully replicate the said environments inside the test laboratory. For this purpose special equipment are available which are complex and very expensive.

The environments experienced during launch are mainly random in nature with a multi-axis configuration with a certain fixture impedance due to attachment to supporting structures. On the other side, the in-flight situation has multi-axis excitation with free boundary conditions.

However, the current test methods often fail to replicate the environments experienced by the said structures since they are mainly single axis tests which tend to have a very high mechanical impedance. The author of this thesis found a significant gap in the testing methods available since there is a lack of a method that incorporates multi-axis testing and fixture apparatus capable of replicating the environments in question.

Hence, based on the case study done by the author a detailed analysis of the existing classical test methods and the novel method of IMMAT suggested in the [Dab14] PhD thesis is given along with a MATLAB simulated example of a simplified application of it.

## 3.2 Classical Vibration test methods

Critical structures are the structures whose failure can lead to detrimental effects like loss of life, financial losses and many more. The structure in interest for vibration behavior can be the whole system in question or a sub system. For example of a satellite, it could be the entire satellite along with the launch vehicle or one of its delicate parts like the solar panel or the antenna which can be more susceptible to vibration generated damages.

All the space structures in concern are tested numerous times through physical tests and simulations. After which the structural integrity of the system is guaranteed. However, after all these steps to prevent errors structures still tend to fail, but with a lower probability of occurrence thanks to advanced testing and quality control techniques.

### 3.2.1 Boundary Conditions

When designing a vibration test for a critical structure a significant focus should be given to the **Boundary conditions** in question. In terms of a satellite launched into space the boundary conditions can be '**Free**' or '**Coupled**'.

In the **free configuration** the structure in concern is not coupled/joint to any other structure. An example include a satellite orbiting in space as in figure 3.1.



**Figure 3.1:** Satellite in space which has free boundary conditions

In the **coupled configuration** the structure is mechanically connected to another structure. Examples include a satellite during its launch and some in-flight stages where it is connected to the launch vehicle, the rocket through

mechanical connections as in figure 3.2. It is important to note that the entire system of the satellite with the launch vehicle is in free boundary condition and the satellite as a separate structure is in coupled boundary condition.



**Figure 3.2:** Satellite in-flight with mechanical attachment to the launch vehicle

### 3.2.2 Excitation Environments

The satellite in its journey to space as discussed previously is mainly facing 3 different excitation environments as Acoustic excitation environment, Aerodynamic excitation environment and Structure borne excitation environments. The most significant effects to the satellite structure happen due to acoustic excitation observed during the launch phase due to the rapid combustion inside the rocket engines.

#### Aerodynamic Excitation Environment

When a structure is subjected to a rapid flow of air on its external surface, it generates distributed excitation forces which are called as aerodynamic excitation.

This aerodynamic environment can induce rapid flow normal to or tangential to the surface resulting in the structure to dynamically respond with random vibration and mechanical shock. An example of aerodynamic excitation include the launch vehicle in-flight, missiles en-route to target and many more.

In this thesis, we are more interested in the random vibration response of the critical structures due to aerodynamic excitation.

The preferred method for simulating an Aerodynamic environment is the use of a wind tunnel. This method is ideal if the structure under observation

is having a coupled boundary condition. However, there are several drawbacks associated with the use of a wind tunnel to simulate Aerodynamic environments as below.

- Incapability to generate wind speeds required to test the full-scale versions of the critical structures in question.
- The structures must be modified and adjusted to accommodate the possible boundary conditions available in the test centre hence resulting in tests which doesn't replicate in-service situations.

However, wind tunnels do give better results in comparison to more tradition test apparatus like shaker systems with electrodynamic or hydraulic origins.

### Acoustic Excitation Environment

An acoustic environment occurs when the structure is excited by a rapid fluctuation of pressures in the air near the surface of the structure.

The acoustic excitation environment occurs mainly during the satellite launch when its booster rockets create compression waves in the nozzle due to the turbulent mixing of exhaust gases with the ambient atmosphere. These waves are then transmitted from the source through atmospheric air to the space structure which results in vibration of the launch vehicle and the satellite. Mainly these vibrations are random in nature.

Furthermore, a rocket launch can be termed as a situation of only acoustic excitation environment at high frequencies above 50Hz.

Acoustic environments can be classified into 2 main subsections as

- Propagating Wave Environment
- Reverberating Acoustic Environment

For **Propagating Wave Environment** where the acoustic wave propagates only in one direction we use a *propagating wave facility*. These facilities are very expensive in nature and is mainly used by top tier institutions like the National Aeronautics and Space Administration(NASA).

A **Reverberating acoustic environment** occurs when the resulting sound waves are reflected resulting in a diffused sound field. A good example, is at the launch of the satellite where the propagating wave environment is reflected back

through the support structures, surrounding buildings etc., Significant effort is made to ensure that this reverberant acoustic environment is suppressed during launch. This topic is not a part of this thesis hence is not discussed here. If required read the resource [Pan14].

The figure 3.3 is depicting the acoustic environment observed during a rocket launch.

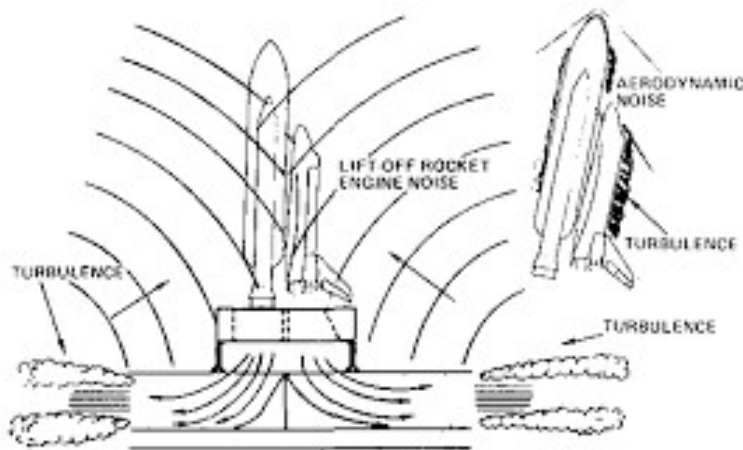


**Figure 3.3:** Acoustic vibration environment of a Rocket Launch [Pan14]

The best solution to simulate a reverberant acoustic environment is an acoustic reverberation chamber. It consists of a large chamber with thick reflective walls. Usually during testing, we introduce noise using chamber air modulators with microphones to measure the noise. Mostly due to the cost associated with propagating wave facilities, for both acoustic environments we use Acoustic reverberant chamber. However, for simpler test requirements there are cases where acoustic environments are replicated using electrodynamic and hydraulic shaker systems.

### Structure-borne Excitation Environment

Structure-borne excitation occur when one structure is excited by another structure in vibration which are connected through a mechanical coupling or a contact area. Structure-borne excitation can be oriented in one axis or in multi-axis depending on the source of excitation. During the process of transportation of

the space vehicle from the production site to the launch site it can undergo significant amount of structure-borne vibration. Often, before in the 20<sup>th</sup> century this phase of satellite launch procedure was neglected which resulted in unseen failures.

Structure-borne vibration can result in random, sinusoidal or transient vibrations. The state-of-the-art for Structure-born excitation environment is the use of a single or multi-axis test facility with an impedance matching fixture. The fixture apparatus configuration is a very important parameter here because its responsible to simulate the mechanical coupling or contact area of the structure-borne excitation environment.

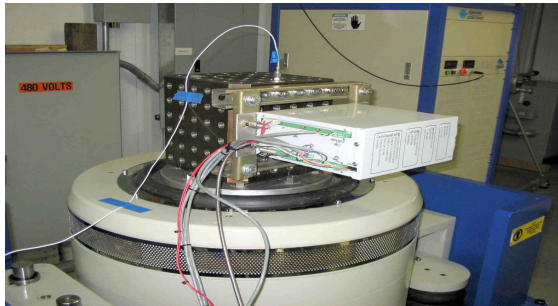


Figure 3.4: Electrodynamic Shaker conducting a classical vibration test

As depicted in figure 3.4 a classical vibration test can reveal a lot of information about the device in terms of its vibration response. However, it has its own limitations.

The shaker typically has very high mechanical impedance and by attaching the structure under investigation to it, we seriously alter the structure's dynamics which mostly leads to severe over-testing and occasionally some under-testing. For a structure like a rocket in-flight which is having free boundary conditions the alteration of dynamics is much severe, which can lead to failures which are significantly unrealistic.

This dissimilitude between the in-service environment and the laboratory environment with respect to the mounting impedance is called the **impedance mismatch** problem.

Also the classical vibration test has the ability to excite the structure in only one axis of motion. In the in-service environment the excitations are generally multi-axis in nature.

On top of this, the excitation initiation location can be quite different to laboratory locations since laboratory fixtures have limited capability. This is particularly true for aerodynamic and acoustic excitation environments where forces are distributed over the external surface of the structure.

### 3.3 Mounting impedance

Generally in classical vibration tests we design fixtures to be very stiff in order not to have any natural frequencies within the frequency range of the test. Through this approach we give rise to a new problem which is the **Impedance mismatch**. Even with a very stiff fixture we still get natural frequencies of the fixture in the frequency range of the test. This will result in the fixture vibrating, resulting in more vibrations transferred at the anti nodes of the fixture and less vibrations transferred at the nodes of the fixture which will result in an unrealistic environment from the actual one.

#### 3.3.1 Advanced Fixtures

As discussed above a fixture is designed to be very stiff to ensure that it has no natural frequencies in the range of the frequencies of the vibration test. The problem with this approach is that it gives rise to the *impedance mismatch* problem.

In order to overcome this impedance mismatch problem in the classical vibration tests, we develop advanced fixtures which fall in the 2 below categories as per [Dab14].

- Multi modal fixtures
- Impedance-matching fixtures

A multi modal fixture in definition is a fixture designed to have natural frequencies within the frequency range of the test. It has been shown that these fixtures offer a far better impedance-match when compared to the classical stiff fixture. However, these fixtures are not often used today due to the time and cost associated in designing and manufacturing them.

An Impedance matching fixture is designed so that the laboratory impedance level matches with the in-service impedance levels.

An impedance matching fixture permits rotational degrees of freedom which are generally locked in the classical stiff fixture. Because of this we have a similar in-service impedance generated.

Even though with the above mentioned advances in fixtures, the industry still prefers classical stiff fixtures since its cheaper and easily accessible.

### 3.4 Impedance Matched Multi Axis Testing

The current technologies in vibration testing considers excitation facility as the important constituent and the structure adopts to accommodate the testing facility during testing. But the suggested novel technologies consider the test structure to be important and tries to adjust the testing apparatus as per the structure to be tested.

The current benchmark in vibration testing is capable of addressing only one of the major issues discussed above at a time. They either match the mounting impedance or the multi directional aspect of the vibration, but not both simultaneously. Hence in this section, we discuss a new method as proposed by [Dab14] which tackles both issues simultaneously. This method is capable of having multi-exciter and advance fixtures capable of successfully having an impedance match simultaneously.

When it comes to impedance matching for conditions with coupled boundary conditions, this new approach tries to have the fixture impedance in match to the in-service impedance between the structure and its environment.

As an example for a case with free boundary conditions, the structure effectively has zero impedance and it is matched by suspending the structure using a soft bungee. Furthermore, any attached exciter should not affect the structures dynamics significantly.

In *IMMAT* method, we give consideration into the load path and axis of excitation in the in-service conditions. Based on this, a suitable multi axis or a single axis apparatus is used to excite the structure. The excitation can be in multi axis or in a single axis orientation as per the in-service situation.

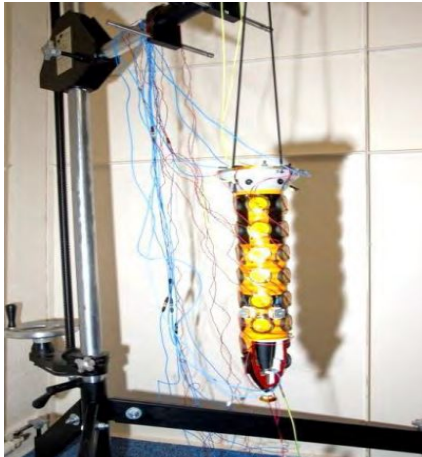


**Figure 3.5:** Model of a Rocket suspended by soft elastics replicating free boundary conditions [Dab14]

## 3.5 Numerical Simulation of a Impedance-Matched Multi Axis Test

### 3.5.1 Introduction

This numerical simulation will use a 5 Degree of Freedom system to replicate a multi-axis laboratory test in MATLAB. The structure is suspended using a soft bungee as in figure 3.6. There are 3 shakers  $Q_1, Q_2, Q_3$  attached to DOF 1, 3 and 5 using flexible drive rods. 3 accelerometers are used to take measurements of the structure's motion and they are attached to DOF 1, 3 and 5 respectively. The shakers and accelerometers are located at the respective degrees of freedom and no special consideration is given to their placing as of now. We assume that the bungee, shakers and the accelerometers do not significantly affect the dynamics of the structure in consideration (ie. They have zero dynamic impedance). We further assume that the entire system only move in the X direction for all 5 DOFs in consideration.

*In the below figure 3.6  $Q_1, Q_2$  and  $Q_3$  are shakers connected to DOF 1, 3 and 5  $A_1, A_2, A_3$  are accelerometers connected DOF 1, 3, 5 and  $M_1, M_2, M_3, M_4, M_5$  are the 5 masses of the system.*

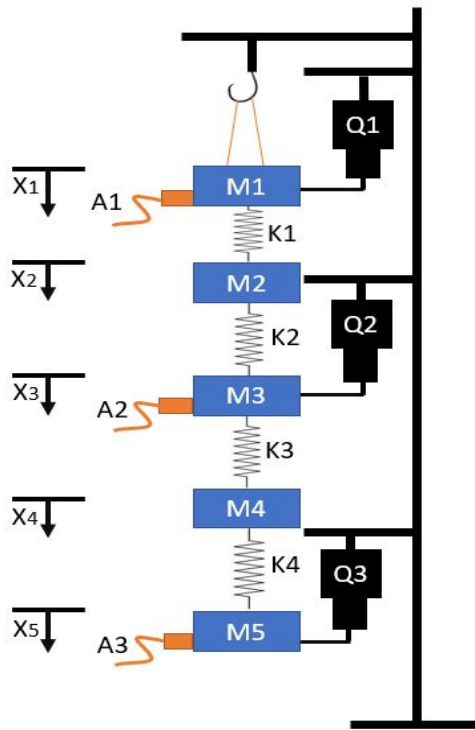


**Figure 3.6:** Impedance Matched Test of a 5 DOF freedom system with 3 shakers to generate excitation and 3 accelerometers to take readings

### 3.5.2 System Parameters, Mass Matrix and Stiffness Matrix

The masses of the system and the spring constants of the springs were set at these given values.  $M1=1$  kg,  $M2=3$  kg,  $M3=1$  kg,  $M4=1$  kg,  $M5=2$  kg,  $K1=2000$  N/m,  $K2=1000$  N/m,  $K3=8000$  N/m,  $K4=6000$  N/m.

$$M = \begin{bmatrix} M1 & 0 & 0 & 0 & 0 \\ 0 & M2 & 0 & 0 & 0 \\ 0 & 0 & M3 & 0 & 0 \\ 0 & 0 & 0 & M4 & 0 \\ 0 & 0 & 0 & 0 & M5 \end{bmatrix} \quad (3.1)$$

$$K = \begin{bmatrix} K1 & -K2 & 0 & 0 & 0 \\ -K1 & (K1 + K2) & -K2 & 0 & 0 \\ 0 & -K2 & K2 + K3 & -K3 & 0 \\ 0 & 0 & -K3 & K3 + K4 & -K4 \\ 0 & 0 & 0 & -K4 & K4 \end{bmatrix} \quad (3.2)$$

Based on these M and K matrices and the **Eigenvalue Problem Equation** defined in 2.11 we obtain the Natural frequencies and Mode Shapes of the system in MATLAB as below.

**Natural Frequencies are 22.8 Hz,11.5 Hz,7.8 Hz,4 Hz and 1.55 Hz respectively.**

The 5 Mode shapes are as below with each column indicating a mode shape.

$$\begin{bmatrix} 0.0006 & -0.0253 & 1.0000 & -0.2944 & -0.7318 \\ -0.0118 & 0.0823 & -0.4492 & -0.5607 & -1.0000 \\ 0.6927 & -1.0000 & -0.0469 & -0.9328 & 0.3644 \\ -1.0000 & -0.4783 & 0.0178 & -0.9682 & 0.5060 \\ 0.1708 & 0.6362 & 0.0967 & -1.0000 & 0.6415 \end{bmatrix}$$

### 3.5.3 Time Domain Response of the System

The obtained system was excited using a mixture of uncorrelated signals of various frequency values using the shaker system and the resulting time domain signals are obtained and plotted using MATLAB. In figure 3.7 the time domain response X1 of mass 1 is shown. These responses will be later used for Frequency Response Plot generation. The responses are plotted with the use of the Ordinary Differential Equation toolbox in Matlab.

### 3.5.4 Frequency Response Functions of the system

Based on the 3 shakers and the 3 acceleration measurements, I obtained 9 FRF plots which is given in figure 3.8. Also the FRF phase plot obtained for shaker Q1 input and accelerometer A1 is given in figure 3.9. The Mathematics and Equations relevant for the observation will be followed in the next chapter. The formulae used to obtain plots 3.8 and 3.9 are based on equation 4.11. It is clear from all plots that resonance oscillations are observed at the natural frequencies calculated in the previous section at 22.8 Hz,11.5 Hz,7.8 Hz,4 Hz and 1.55 Hz values.

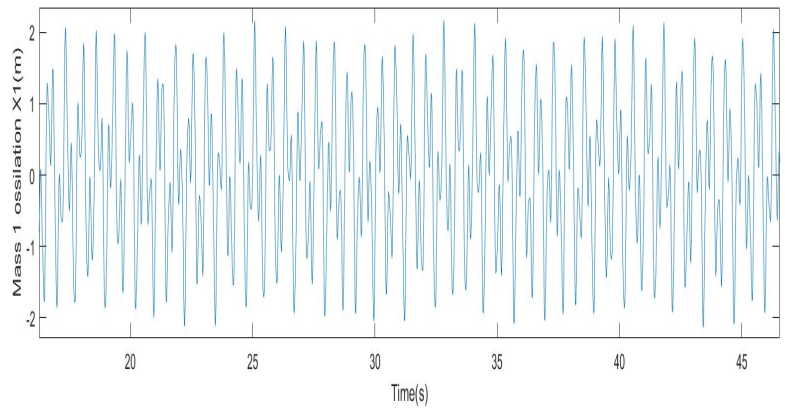


Figure 3.7: Resulting time domain plot of M1

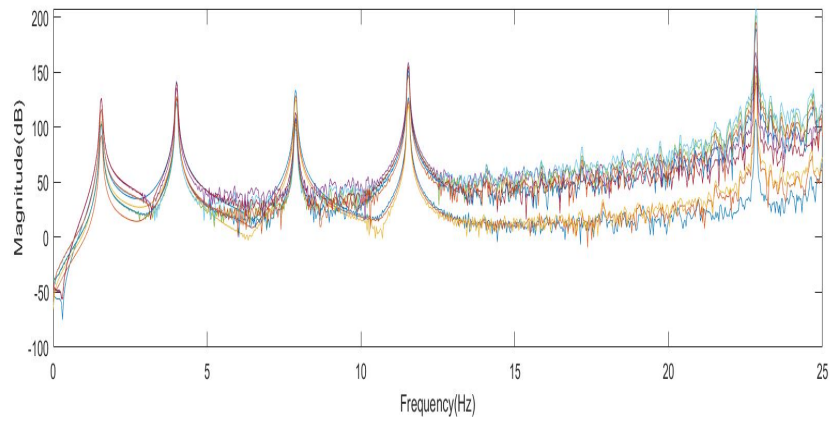


Figure 3.8: FRF Magnitude plots obtained from the data taken from shaker measurements and accelerometer readings

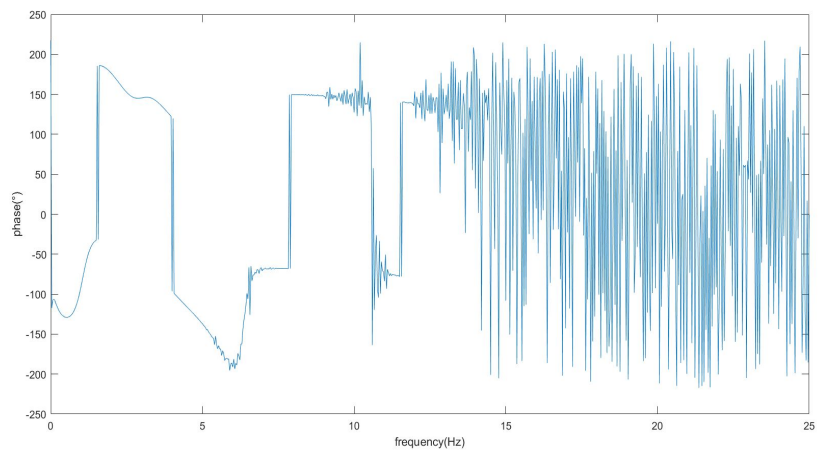


Figure 3.9: FRF Phase Plot obtained from the data taken from shaker Q1 measurements and accelerometer A1 readings

### 3.6 Concluding remarks on Impedance Matched Multi Axis Test

Overall, an IMMAT test can reveal more information about the structure in-service than a classical high impedance single axis test. This is because an IMMAT test can predict the in-service conditions by matching the impedance levels in-service to the laboratory conditions (ex. use of a soft bungee to hang the structure in question to simulate free-free boundary conditions). In addition, the excitation observed in-service is generally multi-directional in nature and the use of a single axis excitation like in the classical test will give failure modes that are unrealistic in practice. But, with multi axis excitation we can combine the individual excitation given by each shaker in consideration to successfully match the frequency spectrum in-service and also the magnitude levels.

However, the costs associated with Multiple shakers and Advanced fixtures needed for IMMAT tests make these tests a lot expensive for general testing needed. Hence, companies are moving towards advanced simulations based on computer software and numerical discretization. However, as per the understanding of the author, for complex problems the costs associated for simulations due to the requirement of advanced computer capabilities and programmer time is quite high. The simulation approach is far more lucrative if its used consistently for Vibration Simulation which will in-turn drive the cost per simulation lower. Hence, in the last part of this thesis, the author mainly focuses on software simulations to analyse the effects of vibrations on critical structures of the satellite.

### 4.1 Introduction

A signal that we encounter can be basically characterised as **deterministic** and as **non-deterministic(random)**. A deterministic signal is a signal whose time history can be predicted and a non-deterministic(random) signal is a signal whose time history cannot be predicted. Below in figure 4.1 is a non-deterministic signal.

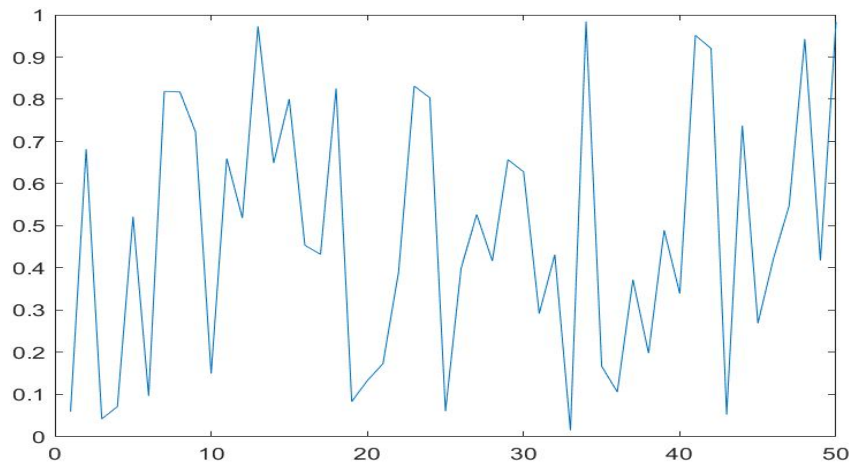


**Figure 4.1:** A time domain plot of a non-deterministic signal generated in MATLAB

A physical example of a non-deterministic signal can be the time history measured from an accelerometer mounted on a car measuring oscillations perpendicular to the ground while the car is in motion. Similarly, pressure fluctuations on the surface of a rocket during launch is also a good example of random vibrations [Pae11].

To analyze and demonstrate the characteristics of such a time history we need new equations and formulae built around probability and statistics. So in this chapter, we shall introduce these formulae relevant for analysis of random

signals in the time and frequency domains. However, the subject of random vibration is quite vast and if the reader wishes to learn more on the topic refer Chapter 14 of [Rao93] and [SK08] for a more detailed definition.

## 4.2 Correlation function of a Random Process

A Random process is said to be a process made out of a collection of random functions  $x_k(t)$ . These random functions are also called sample functions or sample records [Bar12].

In the below figure 4.2 as indicated in chapter 14 of [Rao93] is a Random process with 3 random functions included in the Ensemble.

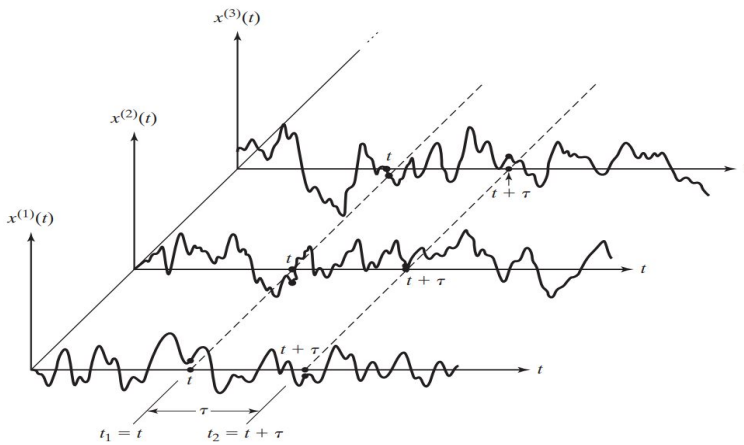


**Figure 4.2:** A random process with 3 random functions

In order to analyse such random signals we introduce some new variables as below.

$$\mu_x(t_1) = E[x_k(t_1)] = \lim_{N \rightarrow \infty} \frac{1}{N} \sum_{k=1}^N x_k(t_1) \quad (4.1)$$

$$R_{xx}(t_1, \tau) = E[x_k(t_1)x_k(t_1 + \tau)] = \lim_{N \rightarrow \infty} \frac{1}{N-1} \sum_{k=1}^N x_k(t_1)x_k(t_1 + \tau) \quad (4.2)$$

where:

- $\mu_x(t_1)$ : Mean Value at time  $t_1$  of the Ensemble
- $R_{xx}(t_1, \tau)$ : Auto-correlation function at time  $t_1$  with a gap or period of  $\tau$

### Random Process analysis in the Time domain

If we consider two random processes  $\{x(t)\}$  and  $\{y(t)\}$  we can measure the similarity between the two functions using the cross correlation function shown below.

$$R_{xy}(\tau) = E[x(t)y(t + \tau)] = \lim_{N \rightarrow \infty} \frac{1}{N-1} \sum_{k=1}^N x_k(t)y_k(t + \tau) \quad (4.3)$$

where:

- $R_{xy}(\tau)$  : Cross-correlation function with gap or period  $\tau$

#### 4.2.1 Stationary Random Processes and Ergodicity

A stationary random process is a process where the probability distributions remain invariant under any shift of the time scale. We can state this mathematically as below.

If the ensemble agrees to the below condition in equations 4.4 for any  $t_1, t_2$  then the ensemble is called **stationary**.

$$\begin{aligned} \mu_x(t_1) &= \mu_x(t_2) = \mu_x \\ R_{xx}(t_1, \tau) &= R_{xx}(t_2, \tau) = R_{xx}(\tau) \end{aligned} \quad (4.4)$$

#### Ergodicity

For a given function in a Random process we can calculate the temporal averages as below.

$$\begin{aligned} \mu_x(k) &= \lim_{T \rightarrow \infty} \frac{1}{T} \int_{-T/2}^{T/2} x_k(t) dt \\ R_{xx}(k, \tau) &= \lim_{T \rightarrow \infty} \frac{1}{T} \int_{-T/2}^{T/2} x_k(t)x_k(t + \tau) dt \end{aligned} \quad (4.5)$$

A stationary process is said to be also ergodic if we can obtain all the probability information from a single sample function and surmise that it is valid for all the functions in the ensemble.

This is true if the ensemble agrees to the two below equations given in 4.6 for any  $k, m$  functions in the ensemble.

$$\begin{aligned}\mu_x(k) &= \mu_x(m) = \mu_x \\ R_{xx}(k, \tau) &= R_{xx}(m, \tau) = R_{xx}(\tau)\end{aligned}\quad (4.6)$$

### Important Observations

- The Units of Cross-correlation is  $(Engineering\ Units)^2$ , if  $\{x(t)\}$  and  $\{y(t)\}$  have units as  $(Engineering\ Units)$
- It is important to note that for a process to be ergodic it should be stationary. A process cannot be ergodic without being stationary.
- For two stationary random processes  $\{x(t)\}$  and  $\{y(t)\}$  we can say that  $R_{xy}(\tau) = R_{yx}(\tau)$
- For a stationary process  $\{x(t)\}$  the auto-correlation function is real and even,  $R_{xx}(-\tau) = R_{xx}(\tau)$

All the above analysis is done in the time domain, but the random processes must also be analysed in the frequency domain in order to develop the frequency response functions between Input and Output pairs.

## 4.3 Random Process Analysis in the Frequency Domain

Any signal can be described as a function that varies with respect to time. However, more data about the signal can be understood by knowing the frequency constituents of the signal under consideration. For this we use the Frequency spectrum of a signal which gives us the range of frequencies contained by a signal.

Below in figure 4.3 is represented a function  $y(t)$  which is a combination of sinusoidal functions of different amplitudes and frequencies as indicated below in equation 4.7. The analysis of this function in the frequency domain is provided in figure 4.4 which reveals its constituent frequency components and respective amplitudes.

$$y(t) = 10 \sin(2\pi 40t) + 5 \sin(2\pi 30t) + 3 \sin(2\pi 20t) \quad (4.7)$$

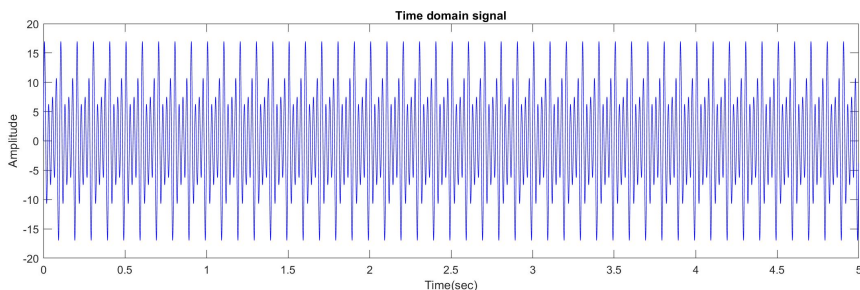


Figure 4.3: A time domain function indicated by equation 4.7

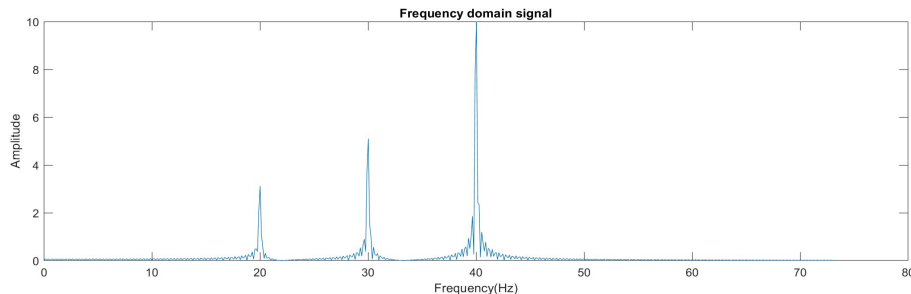


Figure 4.4: The frequency domain plot of equation 4.7

### 4.3.1 Power Spectral Densities

As above in figure 4.4, a signal can be decomposed into a spectrum of frequencies on a continuous range. Such a signal can have its energies concentrated over a certain frequency range or be distributed over the

entire frequency boundary. This analysis about a signal is done using its **Power Spectral Density (PSD)**.

A **Power Spectral Density** of a signal can be defined as the measure of signal's power content versus frequency. There are 2 types of PSD's defined in this thesis as below.

$$S_{xx}(\Omega) = \mathcal{F}[R_{xx}(\tau)] = \int_{-\infty}^{+\infty} R_{xx}(\tau) e^{-i\Omega\tau} d\tau \quad (4.8)$$

$$S_{xy}(\Omega) = \mathcal{F}[R_{xy}(\tau)] = \int_{-\infty}^{+\infty} R_{xy}(\tau) e^{-i\Omega\tau} d\tau \quad (4.9)$$

### Important Observations

- If the variables  $\{x(t)\}$  and  $\{y(t)\}$  are given in units of (*Engineering Units*) then  $S_{xx}$  and  $S_{xy}$  are given in (*Engineering Units*)<sup>2</sup>/Hz.
- $S_{xy}(-\Omega) = S_{yx}(\Omega) = S_{xy}^*(\Omega)$
- $S_{xx}(-\Omega) = S_{xx}^*(\Omega)$

## 4.4 Frequency Response Function

A **Frequency Response Function [FRF]** is a function used to quantify the response of a system to an excitation in the frequency domain.

In Mathematical terms an **FRF** can be described as the Fourier transform of the time domain response divided by the Fourier transform of the time domain input as indicated in the below equation 4.10 where  $X(\omega)$  is a the *Fourier transform of the input  $x(t)$*  and  $Y(\omega)$  is the *Fourier transform of the output  $y(t)$* .

$$H(\omega) = \frac{Y\{\omega\}}{X\{\omega\}} \quad (4.10)$$

However, the actual signals  $x(t)$  and  $y(t)$  are contaminated with noise which makes it difficult to use equation 4.10. In addition to this, the system we measure is quite different from the actual system due to the inherent

individual frequency responses of sensors and filters, effects of quantization of noise, measurement noise and several other noise associated to the test apparatus [MSS05].

Hence, we use estimates of the **FRF** which can predict the **FRF** with high levels of accuracy. In this thesis we deal with 3 such estimates as  $H_1\{\omega\}$ ,  $H_2\{\omega\}$  and  $H_T\{\omega\}$  as indicated below in equations 4.11, 4.12 and 4.13. If the reader needs to gain further knowledge the source [Nui+14] is suggested.

$$H_1(\omega) = \frac{S_{xy}\{\omega\}}{S_{xx}\{\omega\}} \tag{4.11}$$

$$H_2(\omega) = \frac{S_{yy}\{\omega\}}{S_{yx}\{\omega\}} \tag{4.12}$$

$$H_T(\omega) = \frac{S_{yy}(\omega) - S_{xx}(\omega) + \sqrt{(S_{xx}(\omega) - S_{yy}(\omega))^2 + 4|S_{xy}(\omega)|^2}}{2S_{yx}(\omega)} \tag{4.13}$$

**Comments on FRF Estimates**

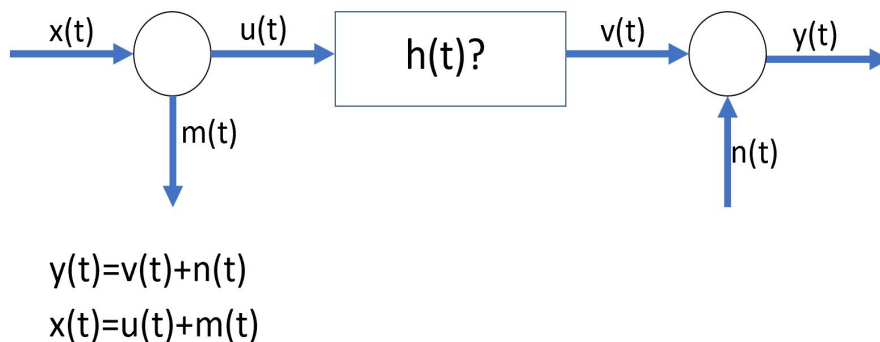


**Figure 4.5:** The effects of noise on FRF measurements

Please refer the figure above in 4.5 to understand the below sections.

As expressed in equation 4.14 the  $H_1(\omega)$  estimate is not affected by the noise in Output. This estimate tends to be **slightly smaller** than  $H(\omega)$  if there is input noise.

$$H_1(\omega) = \frac{H(\omega)}{1 + \frac{S_{MM}}{S_{UU}}} \quad (4.14)$$

The  $H_2(\omega)$  estimate as expressed in equation 4.15 is not affected by input noise. This estimate tends to be **slightly larger** than  $H(\omega)$  if there are errors in the output.

$$H_2(\omega) = H(\omega) \left(1 + \frac{S_{NN}}{S_{VV}}\right) \quad (4.15)$$

### Observations

The above comments are verified by evaluating the below plots. We can see that  $H_1(\omega)$  is almost identical to  $H(\omega)$  when there is only noise in output and  $H_2(\omega)$  is almost identical to  $H(\omega)$  when there is only noise in input [Set+15].

The behaviour of  $H_T(\omega)$  is not discussed in this thesis. However, the author of this thesis came to know that  $H_T(\omega)$  performs well in all cases of [SY02]

- Noise in Input
- Noise in Output
- Noise in Both Input and Output

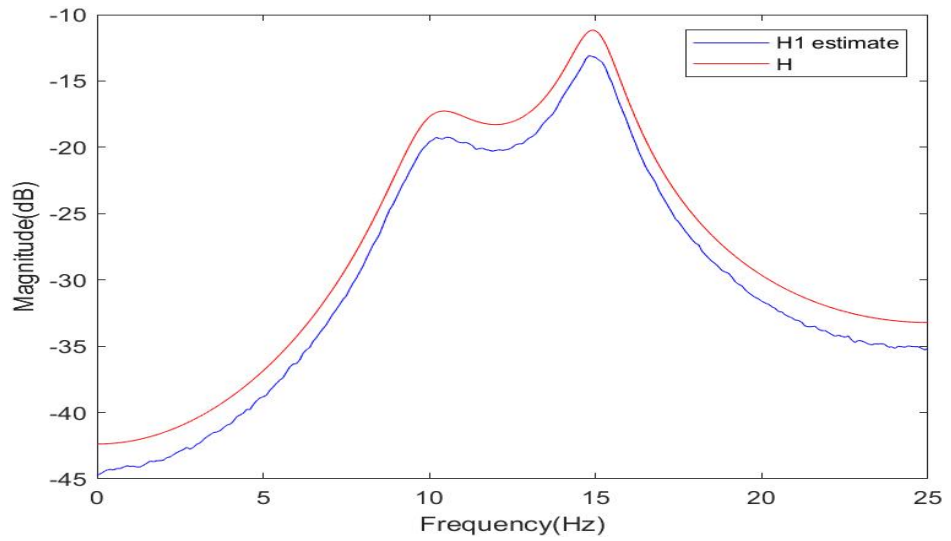


Figure 4.6: Comparison between  $H_1(\omega)$  and  $H(\omega)$  when there is noise in the input signal

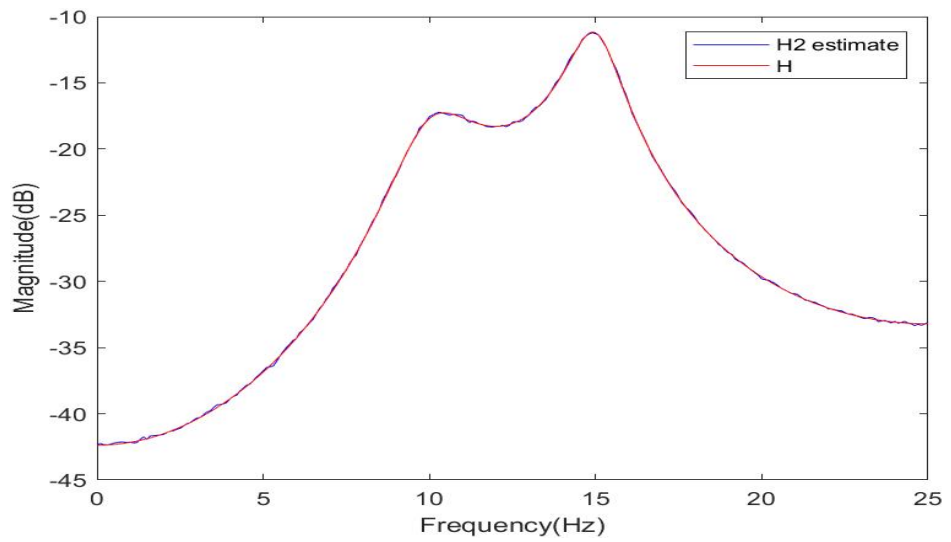
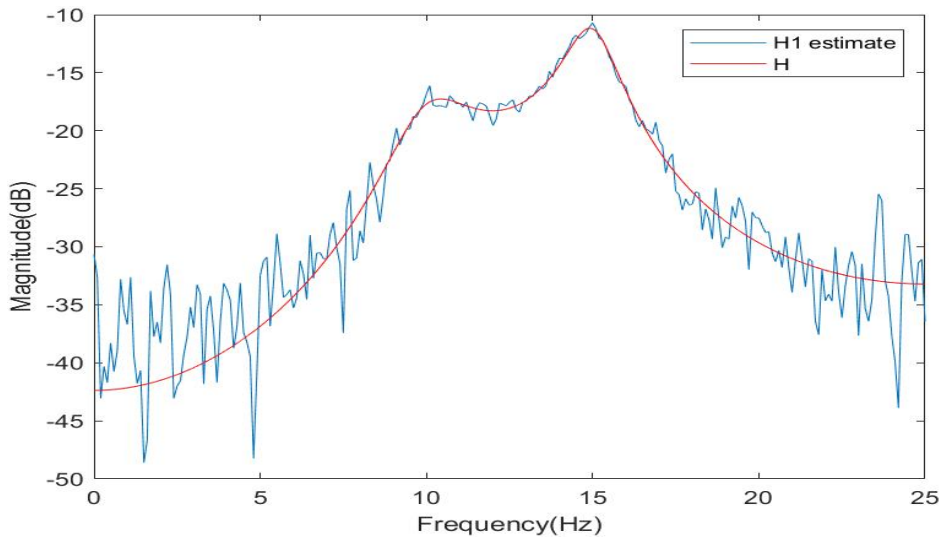
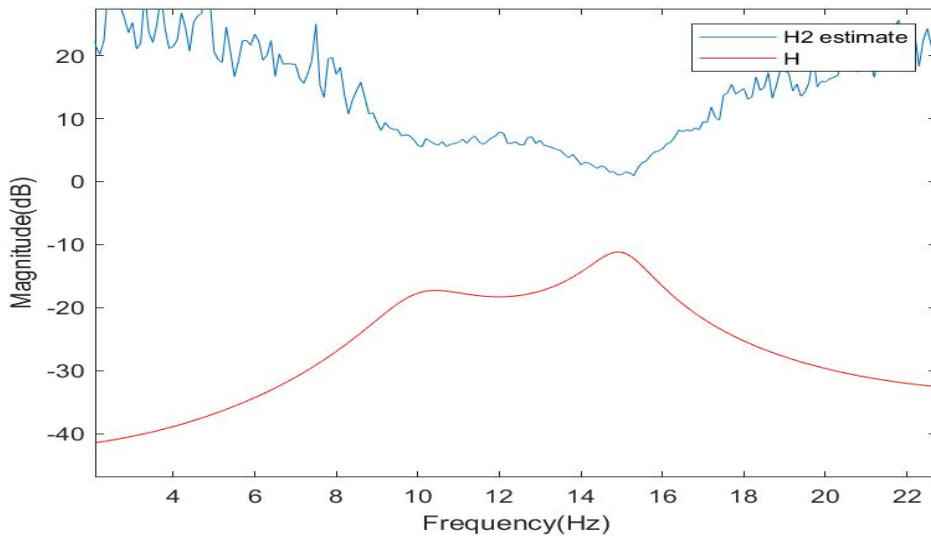


Figure 4.7: Comparison between  $H_2(\omega)$  and  $H(\omega)$  when there is noise in the input signal



**Figure 4.8:** Comparison between  $H_1(\omega)$  and  $H(\omega)$  when there is noise in the output signal



**Figure 4.9:** Comparison between  $H_2(\omega)$  and  $H(\omega)$  when there is noise in the output signal

### 4.5 A Random Excitation Signal

As discussed, a signal can be deterministic or non-deterministic in nature. A signal experienced by the launch vehicle in its flight to the target destination is mainly consisting of non-deterministic (random) excitation components.

In order to evaluate the properties of a Random excitation signal, we simulate such a signal in MATLAB with importance given to the characteristics of the signal without consideration to the magnitudes involved.

The signal generated is indicated in figure 4.10 and the relevant Power Spectral Density is given in figure 4.12 and the Auto-correlation function in 4.11.

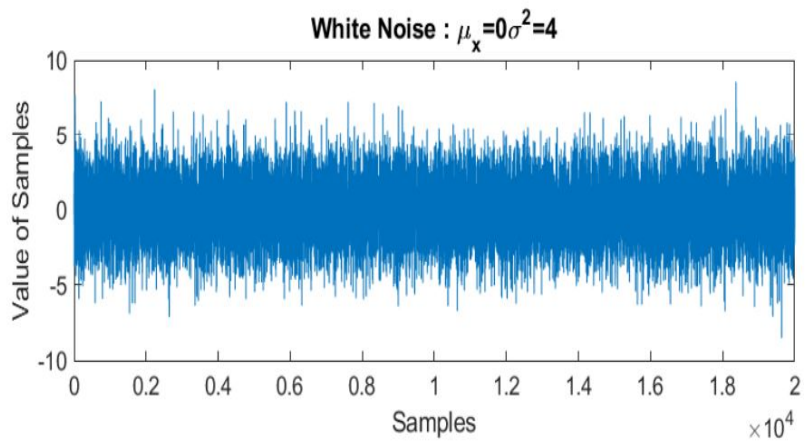
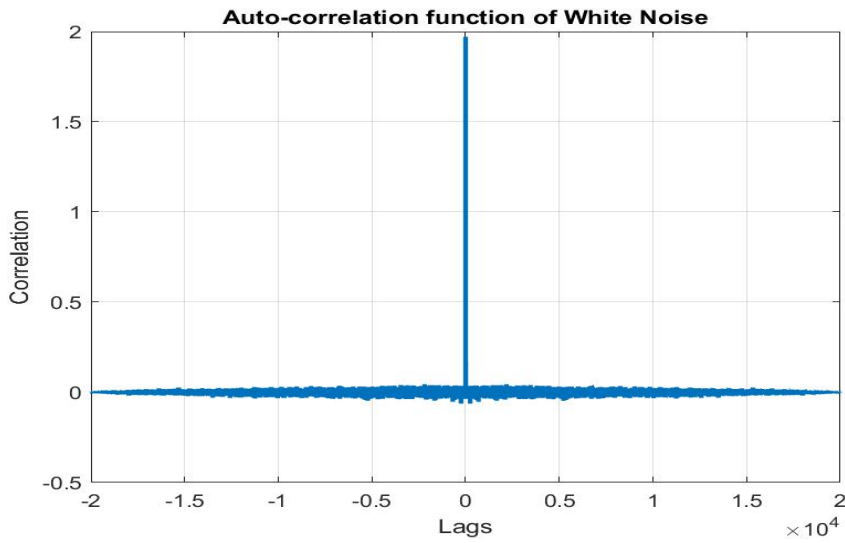
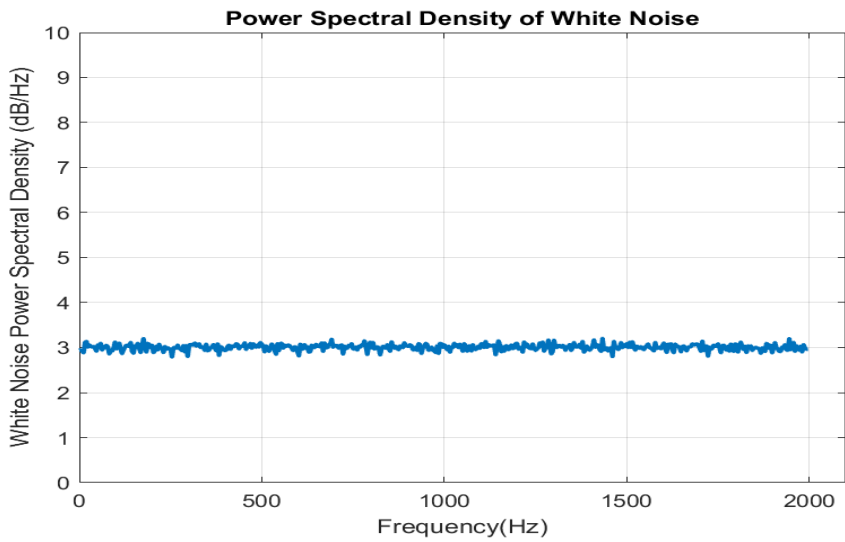


Figure 4.10: White Noise Input



**Figure 4.11:** Autocorrelation function of the White Noise Input



**Figure 4.12:** Power Spectral Density of the White Noise Input

# 5

## Vibration Analysis of a Satellite

---

### 5.1 Introduction

As discussed in the introduction of the thesis, the vibrations transferred to the satellite in the payload area of a rocket can be of various nature which includes Random vibrations, Sinusoidal vibrations, Acoustic pressures and many more. These vibrations are caused due to the forces originating from Engine Propulsion, Debris collision, Loads due to structural movements, Wind Loads etc. In this part of the thesis, we focus mainly on 2 types of vibrations which are **Random vibrations** and **Sinusoidal vibrations**. The Satellite as the payload is a very delicate device which is susceptible to operation failure if excitation beyond its safety limits are transferred. Here in this analysis, we pay a close attention on the **Satellite antenna** and **Solar Panel**. With the analysis done, we aim to identify the resulting mode shapes and FRF plots when the respective components are subjected to Random and Sinusoidal excitation [Isr14] [Yan+17].

### 5.2 Mode Shapes of a Satellite Body with Antenna Structure

For the initial parts of the analysis, a model of a satellite antenna attached to the body of the satellite was modelled in ANSYS and the resulting mode shapes were analysed. The goal of this analysis is to find out the resonant frequencies of the structure and their respective Amplitudes and Mode Shapes.

The simulations done in ANSYS was set to model the below indicated test apparatus as depicted in figure 5.1 which is available in the Mechanical Engineering Department of the University of Twente, Netherlands.

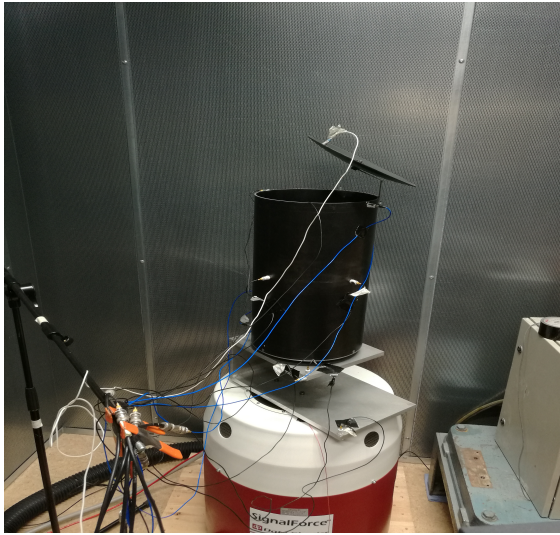


**Figure 5.1:** Replication of a Satellite with Antenna mounted on a Single Axis Exciter

However, the modelled system has some dimensional variations and it has the below material properties as indicated in table 5.1 and dimensions as indicated in table 5.2.

Material Property	Value
Density	$\approx 7850kg/m^3$
Young's modulus	$\approx 210000MPa$
Poisson's ratio	0.30
Shear Modulus	$\approx 81000MPa$

**Table 5.1:** Material Properties of Structural Steel used for modelling the system in ANSYS

Dimensions	Value
Cylinder Diameter	273mm
Cylinder Height	500mm
Cylinder Thickness	4mm

**Table 5.2:** Cylinder Properties of the modelled system in ANSYS

The antenna is modelled using the equation  $\frac{x^2}{4} + \frac{y^2}{2} = 1$  and revolving the line for 360°.The figure of the resulting system is provided below in 5.2.

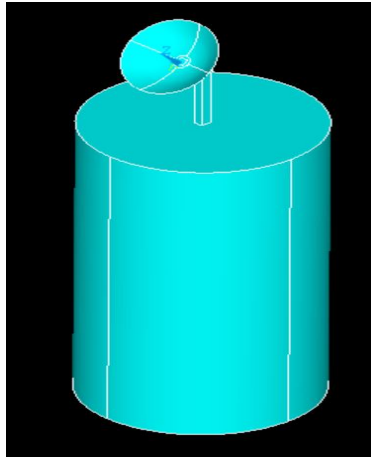
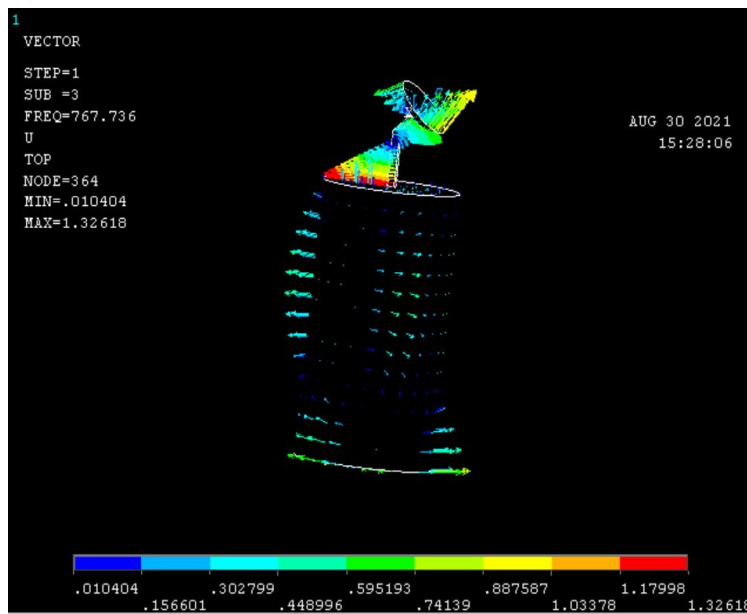


Figure 5.2: Satellite with Antenna system modelled in ANSYS

The connection between the Cylinder and the Antenna is modelled using **Bonded contacts** available in ANSYS. Refer the source [Sun21] for more information about available contact types. Below in the table 5.3 the Natural Frequencies derived from the simulations in the range from 750Hz to 1200Hz are provided. The Vector Plots of the resulting mode shapes for frequencies **767.74 Hz** and **1191.3 Hz** are provided in figures 5.3 and 5.4 respectively. Furthermore, the author of this thesis found out that the type of contacts used significantly effect the resulting mode shapes and natural frequencies as predicted using the simulations.

Mode Number	Modal Frequency(Hz)
1	766.87
2	767.55
3	767.74
4	847.04
5	847.07
6	1060.1
7	1062.6
8	1131.4
9	1191.3
10	1191.7

**Table 5.3:** Modal Frequencies of the Satellite Body with Antenna Structure



**Figure 5.3:** Mode Shape for frequency 767.74 Hz of the Satellite with Antenna system modelled in ANSYS

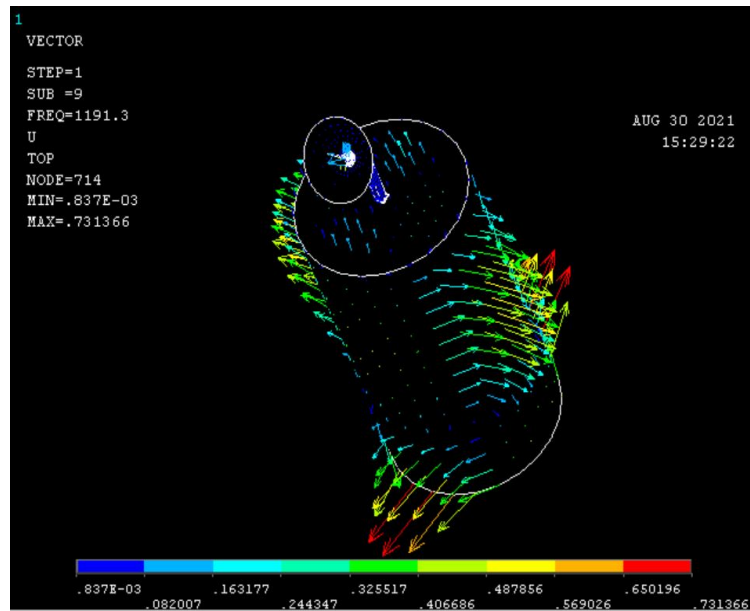


**Figure 5.4:** Mode Shape for frequency 1191.3 Hz of the Satellite with Antenna system modelled in ANSYS

### 5.3 Mode Shapes of the Cylinder available in the laboratory Model depicted in figure 5.1

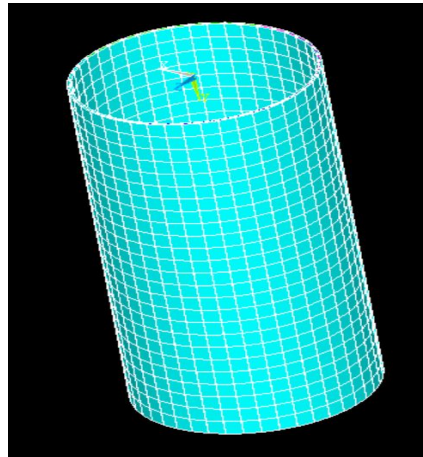


**Figure 5.5:** Discretized model of a cylinder as depicted in ANSYS

The discretized model of cylinder as depicted in figure 5.5 with the same material properties and dimensions as given in tables 5.1 and 5.2 was modelled in ANSYS and the resulting modal frequencies are as depicted in table 5.4 which is given below.

Mode Number	Modal Frequency(Hz)
1	829.51
2	854.65
3	1079.7
4	1108.8

**Table 5.4:** Modal Frequencies of the Cylinder

As depicted above we have 4 modal frequencies in the frequency range 750Hz to 1200Hz. It is important to state that the ANSYS simulation revealed 8 modal frequencies in this range with 4 modal frequencies being

repetitions due to the associated symmetry of the cylinder structure. Hence they are not included in the above table in 5.4.

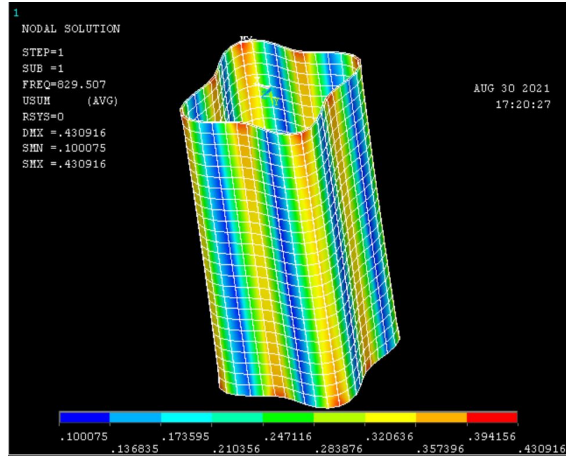


Figure 5.6: Mode Shape of Cylinder at 829.507Hz

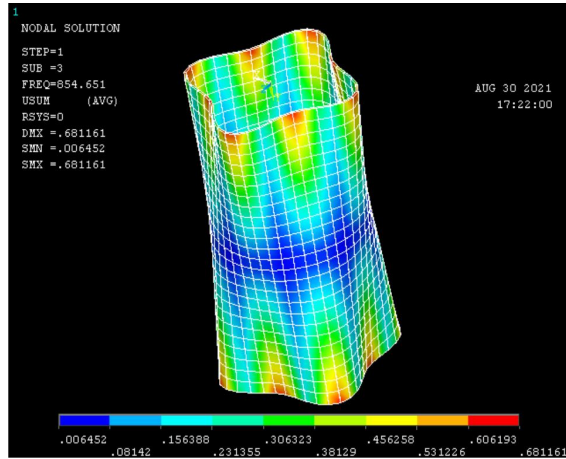


Figure 5.7: Mode Shape of Cylinder at 854.651Hz

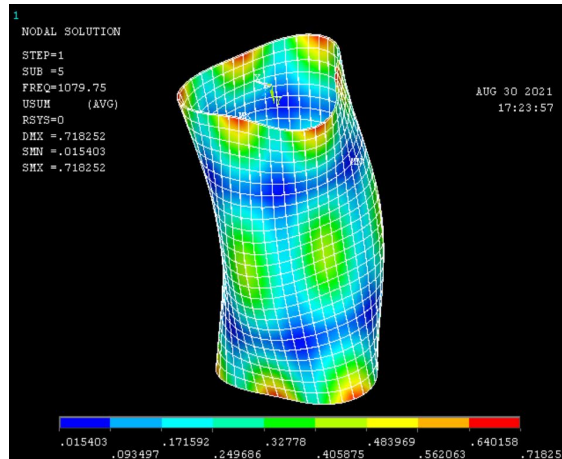


Figure 5.8: Mode Shape of Cylinder at 1079.75Hz

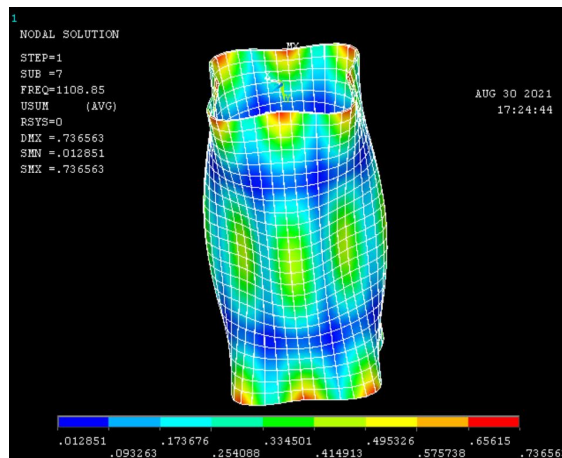


Figure 5.9: Mode Shape of Cylinder at 1108.85Hz

### 5.3.1 Harmonic Analysis of the Cylinder available in the laboratory Model depicted in figure 5.1

A harmonic analysis is done to determine the response of the system under a steady-state sinusoidal(harmonic) loading at a given frequency. In this analysis the excitation frequency is known and is set at a selected

value. By conducting a harmonic analysis we can evaluate the behavior of the structure in the frequency domain.

For our Simulation we use a 1000N force aligned in the  $-Y$  direction which is swept from 700Hz – 1200Hz. The resulting Amplitude and Phase plots of the FRF is presented in figures 5.10 and 5.11 respectively. The FRF plots reveal resonance at 855Hz, 1080Hz and 1109Hz with high amplitude oscillations and phase changes. These frequencies are very close to the modal frequencies as given in table 5.4 which confirms the obtained modal analysis.

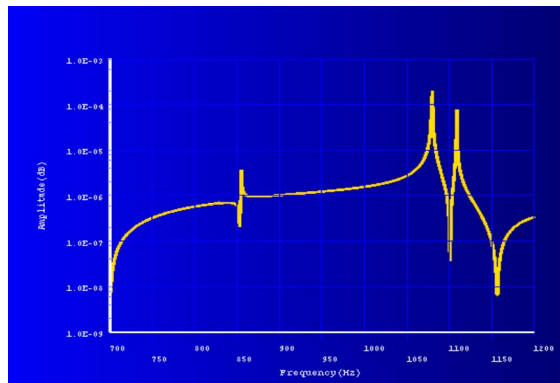


Figure 5.10: FRF Amplitude plot of the resulting Harmonic Analysis

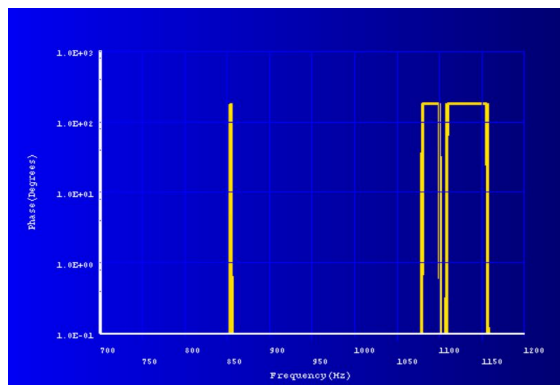


Figure 5.11: FRF Phase plot of the resulting Harmonic Analysis

## 5.4 Vibration Analysis of a Satellite Solar Panel

### 5.4.1 Introduction

Solar panels are an essential part of the satellite and it transforms Sun-light into Electrical power and provides power for the operation of the satellite. The Electrical power generated by the solar panels charge the batteries in the satellite. A typical construction of a Solar Panel is given in figure 5.12 as provided in [Sva20].

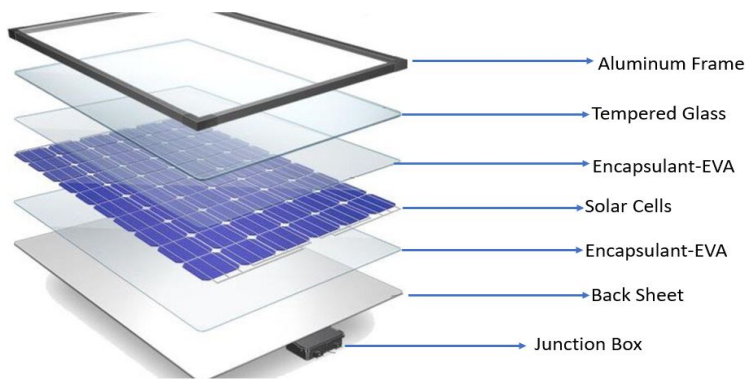


Figure 5.12: Construction of a Solar Panel

Until the early 1990's, space exploration mainly used **Crystalline Silicon Solar panels**. But since the early 1990's a shift towards **Gallium Arsenide based solar panels** occurred due to their higher efficiency levels and lower potential for degradation due to the harsh environments in space.

In the analysis provided in this thesis the solar panel model consists of a **Mono-crystalline Silicon Solar Cells**. In addition, the material used are as indicated in table 5.5. The dimensions of the solar panel was set at  $1.5m * 0.5m * 0.05m$ . The discretized model of the satellite is provided in figure 5.13. This model has an Aluminium outer cover and a top and bottom Tempered glass layer along with Solar Cells modelled using the material Mono-crystalline silicon sandwiched between the glass layers.

Material	Young's Modulus(E)[MPa]	Density [ $\frac{kg}{m^3}$ ]	Poisson's ratio
Mon-crystalline Silicon	112400	2340	0.28
Tempered Glass	66000	2270	0.23
Aluminium Alloy	69000	2700	0.33

**Table 5.5:** Properties of the Material used in the Solar Panel

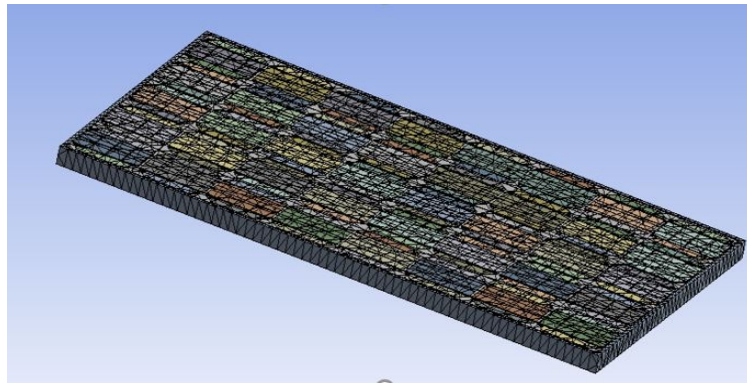


**Figure 5.13:** Discretized model of the Solar Panel developed in SOLIDWORKS

The connection between the Satellite and the Solar Panel was developed by using a fixed end support and the relevant loads are applied on the top and bottom surfaces in the simulations done.

#### 5.4.2 Modal Analysis of the Satellite Solar Panel

The Modal analysis of the modelled solar panel was conducted in ANSYS and 6 mode shapes as given in table 5.6 was obtained in the frequency range from 100Hz to 700Hz.

Mode Number	Mode Frequency(Hz)
1	132.97
2	249.90
3	404.16
4	424.97
5	546.56
6	668.43

**Table 5.6:** Modal Frequencies in the range 100Hz – 700Hz of the Solar Panel developed in ANSYS

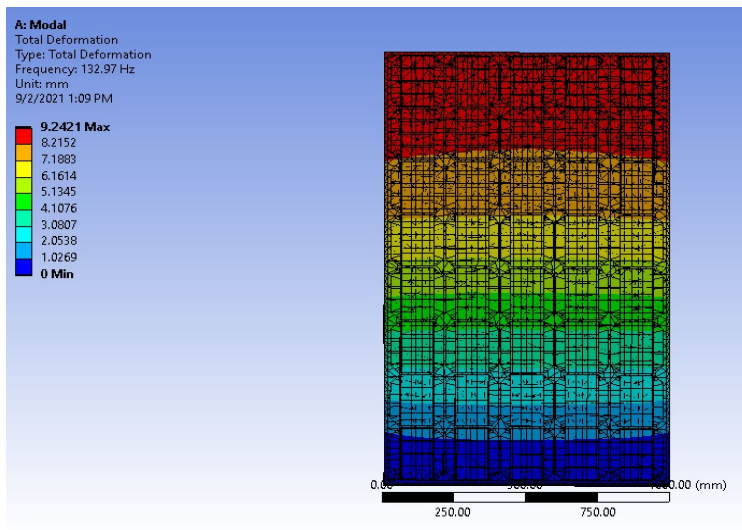


**Figure 5.14:** Mode Shape 1 at 132.97Hz

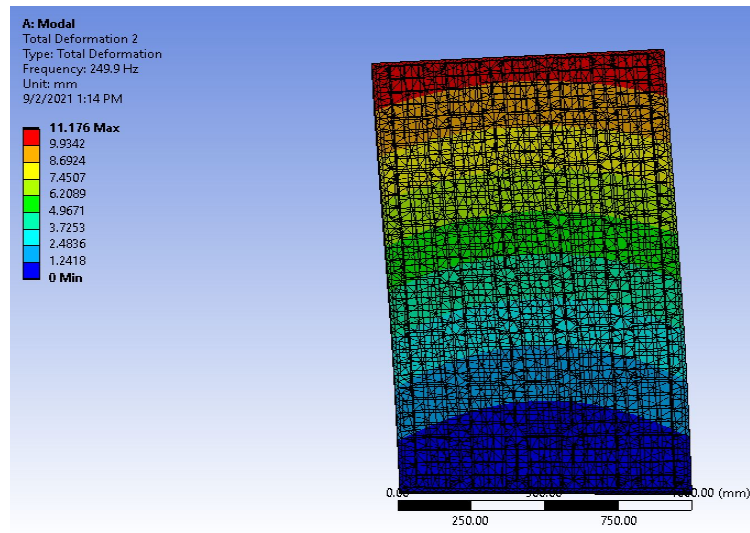


Figure 5.15: Mode Shape 2 at 249.907Hz

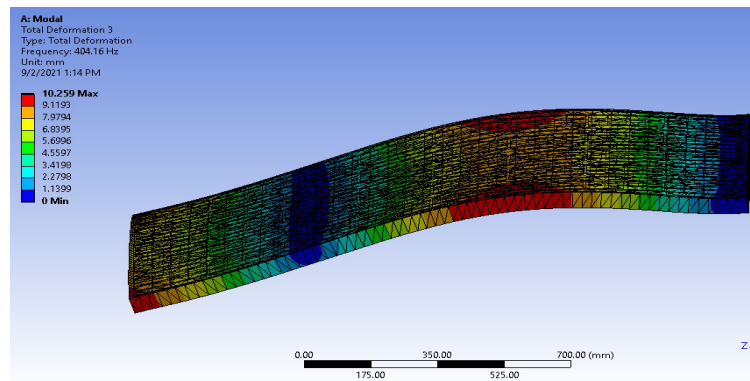


Figure 5.16: Mode Shape 3 at 404.16Hz

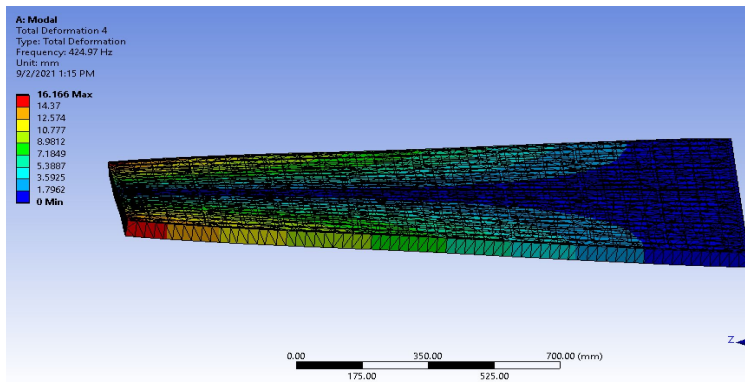


Figure 5.17: Mode Shape 4 at 424.97Hz

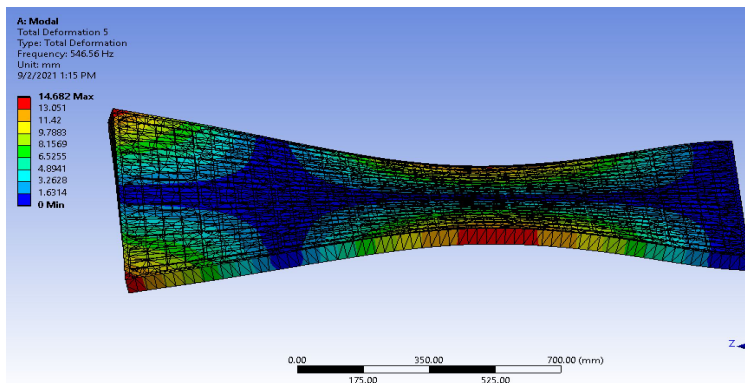


Figure 5.18: Mode Shape 5 at 546.56Hz

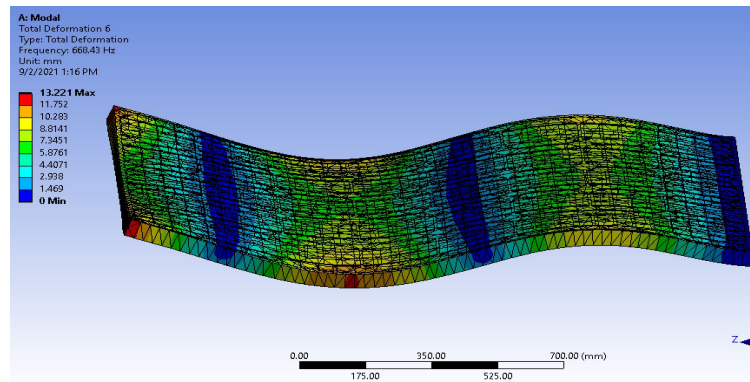


Figure 5.19: Mode Shape 6 at 668.43Hz

### 5.4.3 Random Vibration Analysis of the modelled solar panel in ANSYS

A Random excitation with Acceleration Power Spectral Density as indicated below was applied perpendicularly to the surface of the Solar Panel in the -Y direction. The frequency of this external excitation is in the range of 0-700Hz. The relevant Acceleration Power Spectral Density is indicated as below in figure 5.21.



Figure 5.20: Power Spectral Density of the Acceleration applied in the -Y direction on the solar panel surface

The response of the resulting motion of a point on the top surface of the solar panel on the free-end was recorded and its response Power Spectral Density is plotted in figure 5.21. It is important to note that we get 3 peaks at 3 of the 5 modal frequencies we observed in the modal analysis. The peaks occur near mode 1 at 132.97 Hz, mode 3 at 404.16 Hz and mode 6 at 668.43 Hz.

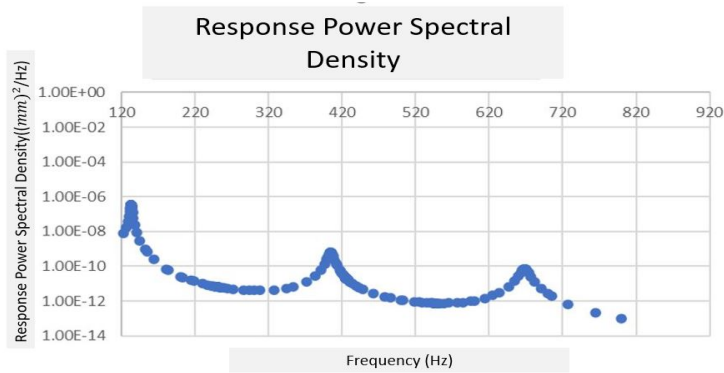


**Figure 5.21:** Response Power Spectral Density of a Point on the free end of the Solar Panel

#### 5.4.4 Harmonic Vibration Analysis of the solar panel

A force of 1000 N in the -Y direction was applied on the top surface of the Solar panel and the force was swept from 1 Hz to 1000 Hz. The resulting response of a point in the free-end of the solar panel was measured. From this data obtained the Frequency response function was observed as in figure 5.22 and 5.23.

As per the analysis conducted resonances were observed at frequencies 132.97 Hz, 404.16 Hz, 668.43 Hz, 830.12 Hz, 900.16 Hz and 973.59 Hz.

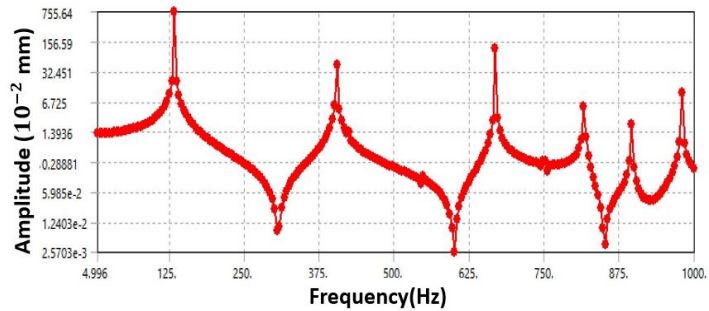


Figure 5.22: Amplitude plot of the Frequency Response Function

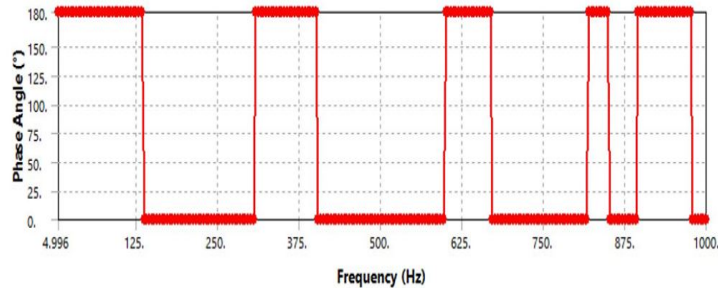


Figure 5.23: Phase plot of the Frequency Response Function

#### 5.4.5 Effect of Step vs Ramp Acceleration on a Solar Panel

A spacecraft with a satellite travelling to space has to overcome a significant gravitational field induced by planet earth. Hence, to overcome this it reaches high amplitude acceleration. As a result of this acceleration, we can experience an onset of vibrations in critical structures like the solar panel and the antenna. Hence, a keen attention has to be made when deciding the flight path of the launch vehicle to limit the Forces applied in order to reduce the on-set of vibrations.

In the below figure 5.24 there is a plot obtained from the flight data from the Space Transportation System 121 as presented in [MK20].

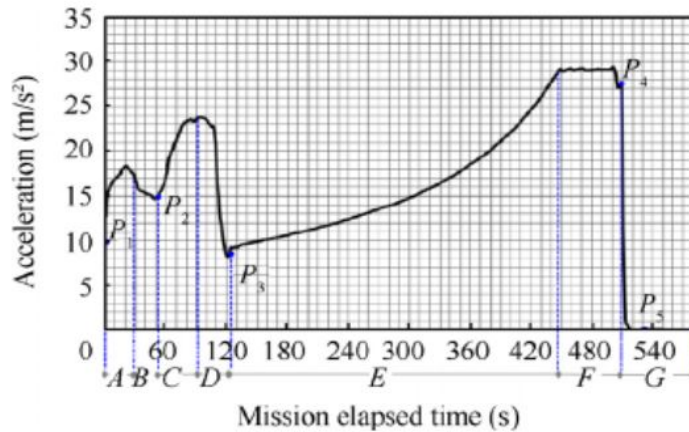


Figure 5.24: Longitudinal acceleration in US Discovery space shuttle, in STS-121 mission

Here in this part of the thesis, we subject the thin plate given in figure 5.25 with dimensions  $1m * 0.2m * 0.01m$  made out of material **structural steel 181** to different acceleration loads as explained below.

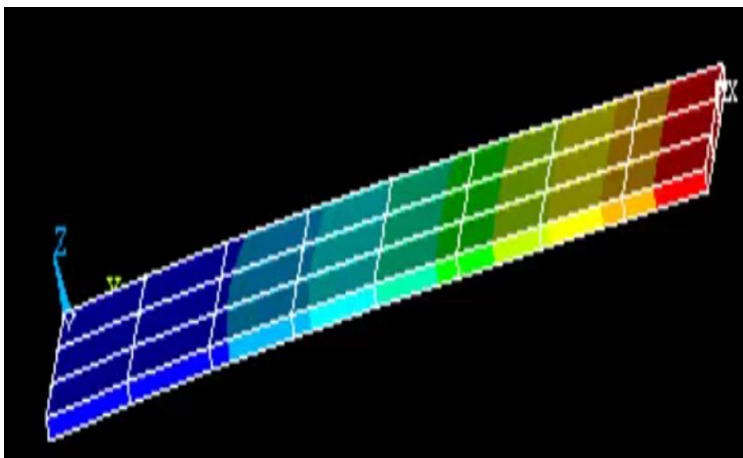


Figure 5.25: The thin plate simulated in ANSYS APDL

Here the measurements are recorded for 10 seconds with the acceleration of  $10\text{ms}^{-2}$  only applied in the interval from 1 to 2 seconds.

### Effect of Stepped Input Acceleration

If you step apply the loads, their values are fully applied at the first substep and remain constant for the remainder of the load step as indicated below in figure 5.26.

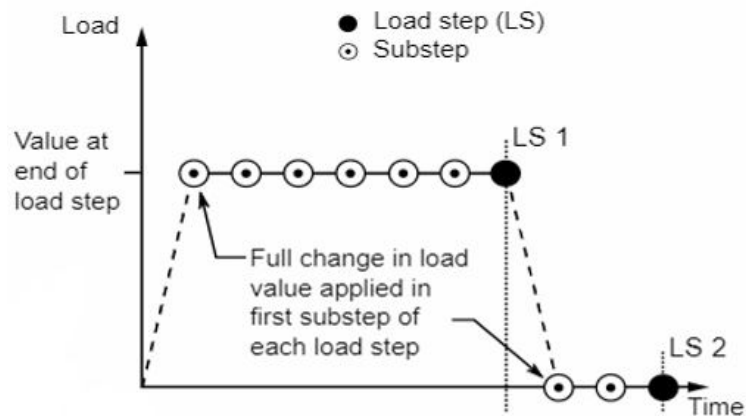


Figure 5.26: Description of a Step Input

The response of a point in the free end of the thin plate is plotted as obtained in ANSYS APDL in the below figure 5.27 and a detailed description of the motion in the initial two seconds is provided in 5.28.

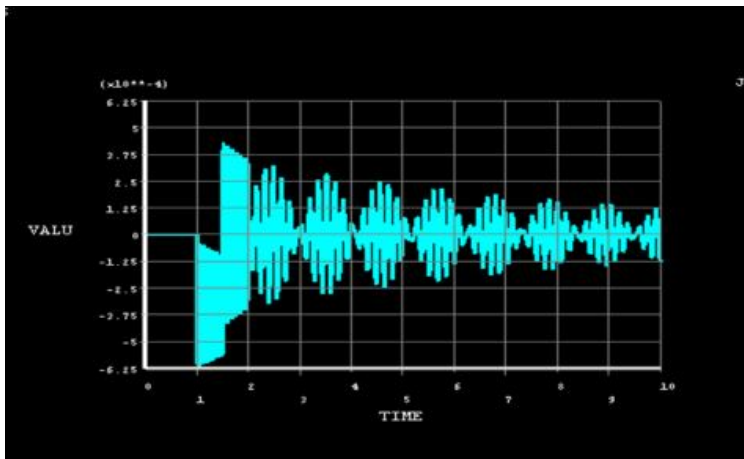


Figure 5.27: Response of a point on the Thin Plate for 10 seconds

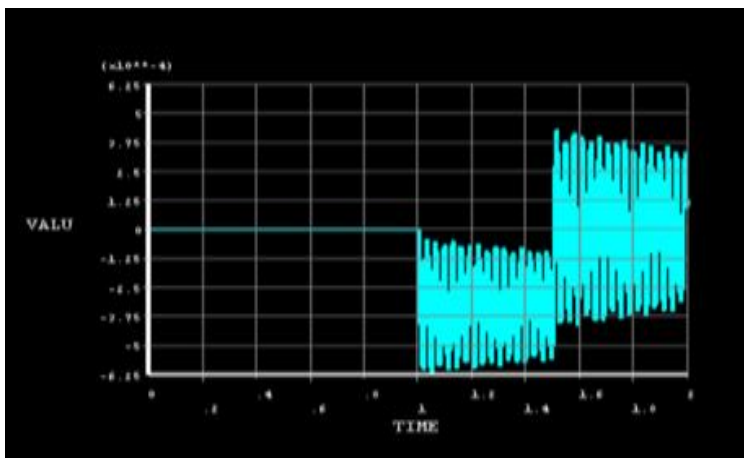


Figure 5.28: Response of a point on the Thin Plate for the initial 2 seconds

### Effect of Ramped Input Acceleration

If you ramp apply the loads, their values are incrementally applied at each sub step in a linearly interpolated fashion, reaching the full values at the end of the load step as indicated below in 5.29.

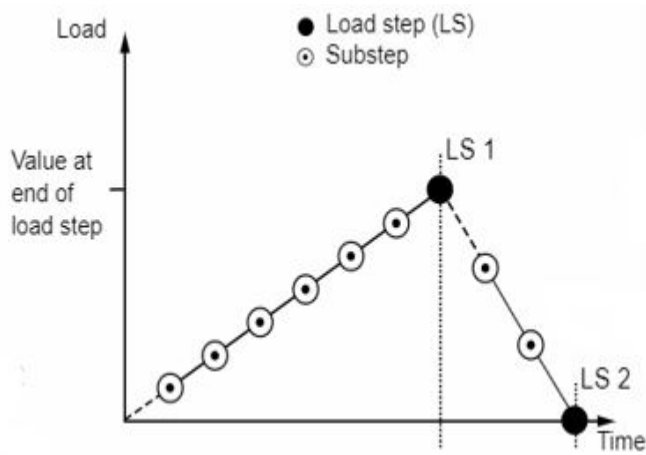


Figure 5.29: Description of a Ramped input

The response of a point in the free end of the thin plate is plotted as obtained in ANSYS APDL in the below figure 5.30 and a detailed description of the motion in the last 8 seconds is provided in figure 5.31.

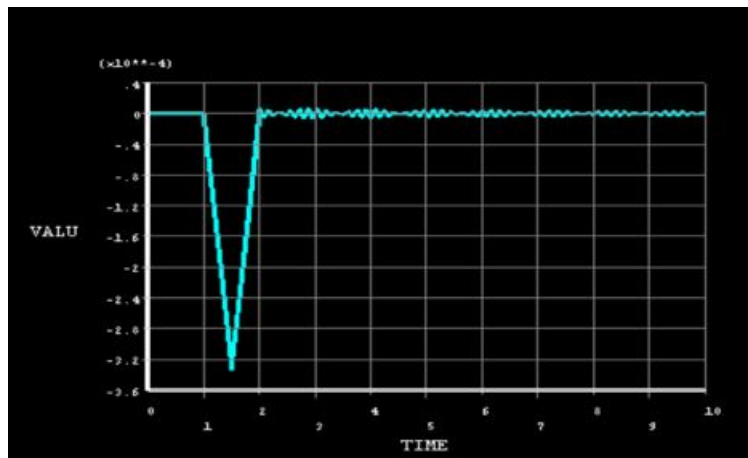
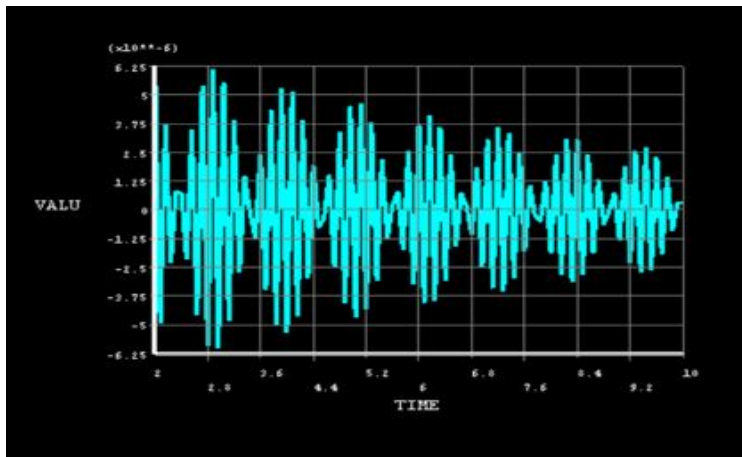


Figure 5.30: Response of a point on the Thin Plate for 10 seconds



**Figure 5.31:** Response of a point on the Thin Plate in the last 8 seconds

### Comments

As seen in both cases of Step and Ramp Accelerations there is a definite onset of vibrations. However, in the case of step input accelerations where the loads are fully applied in the first sub-step the vibration levels are significantly higher than that of the Ramp Input Accelerations. Hence, we can draw a conclusion that a similar behavior would be observed by a solar panel mounted on a satellite during its acceleration profile since both have cantilever plate-like boundary conditions. Therefore, a special attention must be drawn when deciding the accent profile of the space vehicle in relation to vibrations involved. A gradual acceleration profile over a rapid acceleration profile is hence preferred. However, the final decision on the space vehicle path is decided upon close inspection of several aspects like fuel requirements, structural strength to withstand dynamic pressures, payload etc.,

The existing vibration testing of critical structures in the aerospace industry cannot successfully indicate the dynamic properties of the structure under test mainly due to the factors mentioned below.

- Boundary conditions of the critical structures are not replicated in the existing laboratory based tests.
- Load Path of forces applied are not taken into consideration and the tests are limited to single or bi-axial tests at-best which fail to address the multi-axis forces experienced by critical structures.

Hence, a novel method that rectifies the above mentioned issues has to be introduced. Based on this, an approach suggested by [Dab14] named **Impedance Matched Multi Axis Testing** was identified by the author as a superior substitute to the existing techniques. The reasons for the selection of the above mentioned test method was that it aims to match the impedance of the test apparatus to the real conditions as experienced during operation along with implying multi-axis excitation which results in far more accurate revelation of dynamic properties of the structure in consideration.

However, as experienced by the author, vibration testing of highly delicate components of the satellite is a very cumbersome process which require significant expertise and expensive lab apparatus. Hence, there is a growing need in industry to look for other viable methods to predict the dynamic characteristics of critical structures under consideration.

With the advancement of prevailing processor capabilities, computer programming and simulation software, the industry is moving more towards Mechanical Simulations. With this in mind, the simulations conducted on the Critical components of the satellite whose failure is catastrophic revealed valuable information about the structure in-consideration.

For example, the simulations done on the cylinder with antenna structure successfully depicted the failure modes with close proximity to what is observed by vibration testing in a lab setup. Also, the simulations on the satellite solar panel revealed that, it is now possible to geometrically construct the Solar panel using Finite Element and Discretization based softwares with high levels of accuracy in comparison to the actual physical apparatus. Hence, the resulting failure modes would also be able to provide quality dynamic information about the structure in-consideration. All the above stated facts prove that mechanical simulations are capable of successfully producing the information revealed about the structure through physical vibration tests with acceptable accuracy. However, by experience of the author, the best-fit method is to use both methods of vibration testing and mechanical simulations in-tandem to reveal accurate dynamic information about the structure.

As future research, the author suggests a comparison between Vibration Testing and Mechanical Simulations with emphasis given to the quality and accuracy of information revealed with a special attention given to the **Cost of conducting the test procedures**. This is due to the fact that the cost associated is the deciding factor in the modern day testing and simulation procedures and hence must be paid a close attention to as per the experience of the author.

In addition to this, as a further step in this research conducted, a more cost effective methodology to obtain multi-axis excitation could be investigated. The current existing methods rely on the use of multiple exciters, but the author believe that this method is not cost-effective due to the high cost of exciters involved. Hence, suggests development of vibration fixtures capable of converting a single-axis excitation into multi-axis excitation in the frequency range in consideration. This would result in lowering the cost associated with the relevant vibration testing making it a far more cost effective methodology than it is now.

## Bibliography

---

- [08] 27–69. In: *Spacecraft Structures*. Berlin, Heidelberg: Springer Berlin Heidelberg, 2008. ISBN: 978-3-540-75553-1. DOI: [10.1007/978-3-540-75553-1\\_6](https://doi.org/10.1007/978-3-540-75553-1_6). URL: [https://doi.org/10.1007/978-3-540-75553-1\\_6](https://doi.org/10.1007/978-3-540-75553-1_6) (see page 2).
- [AA] National Aeronautics and Space Administration. *Vibration Testing*. Accessed: 2011-07-04 (see page 6).
- [Bar12] John Baren. **What is Random Vibration Testing?** *Sound and Vibration* 46 (Feb. 2012), 9–12 (see page 39).
- [BB04] A.A. Becker and A.A. Becker. **An Introductory Guide to Finite Element Analysis**. Introductory Guide Series. Professional Engineering, 2004. ISBN: 9781860584107. URL: <https://books.google.nl/books?id=-oGEQgAACAAJ> (see page 17).
- [BS16] Anders Brandt and Raj Singhal. **Shock Vibration, Aircraft/Aerospace, Energy Harvesting, Acoustics Optics, Volume 9: Proceedings of the 34th IMAC, A Conference and Exposition on Structural Dynamics 2016**. Jan. 2016. ISBN: 978-3-319-30086-3. DOI: [10.1007/978-3-319-30087-0](https://doi.org/10.1007/978-3-319-30087-0) (see page 9).
- [CMN] Raoul Caimi, Ravi Margasahayam, and Jamel Nayfeh. *Rocket Launch-Induced Vibration and Ignition Overpressure Response*. NASA Kennedy Space Center Florida, USA (see page 2).
- [Dab14] Philip Matthew Daborn. **Smarter Dynamic Testing of Critical Structures**. PhD thesis. University of Bristol, Faculty of Engineering, 2014 (see pages ii, 4, 10, 25, 31–33, 72).
- [Isr14] Asif Israr. **Vibration and Modal Analysis of Low Earth Orbit Satellite**. *Shock and Vibration* 2014 (Aug. 2014), 8. DOI: [10.1155/2014/740102](https://doi.org/10.1155/2014/740102) (see page 50).
- [Knu73] Donald E. Knuth. **1.2**. In: Addison-Wesley, 1973 (see page 10).
- [Lal10] Christian Lalanne, 287–339. In: Jan. 2010. ISBN: 9780470611975. DOI: [10.1002/9780470611975.ch11](https://doi.org/10.1002/9780470611975.ch11) (see pages 5, 10).

- [MK20] Ali Mahmoodi and Isooda Kazemi. **Optimal motion cueing algorithm for accelerating phase of manned spacecraft in human centrifuge-NC-ND license (<http://creativecommons.org/licenses/by-nc-nd/4.0/>)**. *Chinese Journal of Aeronautics* 33 (Mar. 2020), 1991–2001. DOI: [10.1016/j.cja.2020.02.004](https://doi.org/10.1016/j.cja.2020.02.004) (see page 67).
- [MSS05] José M. Simões Moita, Cristóvão M. Mota Soares, and Carlos A. Mota Soares. **Active control of forced vibrations in adaptive structures using a higher order model**. *Composite Structures* 71:3 (2005). Fifth International Conference on Composite Science and Technology, 349–355. ISSN: 0263-8223. DOI: <https://doi.org/10.1016/j.compstruct.2005.09.009>. URL: <https://www.sciencedirect.com/science/article/pii/S0263822305002618> (see page 44).
- [Nui+14] Pieter Nuij, David Rijlaarsdam, M. Steinbuch, and Johan Schoukens. **Introduction to Frequency Response function measurements [part 1: from time to frequency domain; part 2: from signal to system analysis; part 3: frequency domain analysis and performance optimization of nonlinear systems]**. *Mikroniek* (Sept. 2014) (see page 44).
- [OH22] J. Ormondroyd and J.P. Den Hartog. **The theory of dynamic vibration absorber**. *Journal of Applied Mechanics* 50 (1928-09-22) (see page 22).
- [Pae11] Thomas L. Paez. **Random Vibration – History and Overview**. In: *Rotating Machinery, Structural Health Monitoring, Shock and Vibration, Volume 5*. Ed. by Tom Proulx. New York, NY: Springer New York, 2011, 105–127. ISBN: 978-1-4419-9428-8 (see page 38).
- [Pan14] Jayanta Panda. **Aeroacoustics of Space Vehicles**. In: Presentation for Applied Modeling Simulation (AMS) Seminar Series Building N258, Auditorium (Room 127), NASA Ames Research Center Moffett Field, CA, 2014 (see page 29).
- [Pie66] A.G. Piersol. **The development of vibration test specifications for flight vehicle components**. *Journal of Sound and Vibration* 4:1 (1966), 88–115. ISSN: 0022-460X. DOI: [https://doi.org/10.1016/0022-460X\(66\)90156-8](https://doi.org/10.1016/0022-460X(66)90156-8). URL: <https://www.sciencedirect.com/science/article/pii/0022460X66901568> (see page 3).
- [Rao93] Singiresu S. Rao. **Mechanical Vibrations- 2004**. Upper Saddle River: Pearson-Prentice Hall, 1993 (see pages 11, 16, 39).
- [Set+15] Rajkumar Sethu, Alok Bhagat, C. Sujatha, and S. Narayanan. **Comparison of Various Techniques Used For Estimation of Input Force and Computation of Frequency Response Function (FRF) From Measured Response Data**. In: July 2015 (see page 45).

- [SK08] Kihong Shin and Joseph K.Hammond. **Signal Processing for sound and vibration engineers**. West Sussex,England: John Wiley Sons Ltd, February 2008 (see page 39).
- [Sun21] Özgün Sunar. *Ansys Contact Types and Explanations*. 2021. URL: <https://www.mechead.com/contact-types-and-behaviours-in-ansys/> (see page 52).
- [Sva20] Jason Svarc. *Solar Panel Construction*. 2020. URL: <https://www.cleanenergyreviews.info/blog/solar-panel-components-constructions/> (see page 59).
- [SY02] Hideo Suzuki and Michiyuki Yamaguchi. **Comparison of FRF Curve Fitting Methods for the Loss Factor Measurement** (Jan. 2002) (see page 45).
- [WL92] P.L. Walsh and J.S. Lamancusa. **A variable stiffness vibration absorber for the minimization of transient vibrations**. *Journal of Sound and Vibration* 158 (1992) (see page 22).
- [Yan+17] Bo Yan, Ke Wang, Chang-Xi Kang, Xinong Zhang, and Chuanyu wu. **Self-Sensing Electromagnetic Transducer for Vibration Control of Space Antenna Reflector**. *IEEE/ASME Transactions on Mechatronics* 22 (Oct. 2017), 1944–1951. DOI: [10.1109/TMECH.2017.2712718](https://doi.org/10.1109/TMECH.2017.2712718) (see page 50).